Study of the propagation of defects governed by a brutal damage law using a coupled boundary element and level set technique.

Anne-Lise Guilmin

June 25, 2009

Master at	:	Ecole Centrale de Nantes (ECN)
Conducted at	:	Institut de Recherche en Génie Civil et Mécanique (GeM)
Supervisors	:	**Nicolas Chevaugeon, GeM** **Nicolas Moës, ECN**
Jury members	:	**Pedro Diez, Universitat Politècnica de Catalunya (UPC)** **Steven Le Corre, ECN** **Nicolas Chevaugeon, GeM**

Master thesis report
Master of Sciences in Computational Mechanics · Erasmus Mundus program

Abstract

The team of *Institut de Recherche en Génie Civil et Mécanique* (GeM) has developed a brutal damage law to compute the propagation of defects in materials like concrete. In order to test this law on an infinite medium, they wanted to couple the code of propagation with a code using the boundary element method (BEM) which would update the propagation criteria. This criteria takes into account a surface energy which requires to know the gradient of displacement on the boundary. I was in charge to write a BEM formulation able to compute the gradient of displacement on the boundary and to couple it with the propagation code. This work has been done in the frame of my master thesis untitled "Study of the propagation of defects governed by a brutal damage law using a coupled boundary element/level set technique." which was conducted in the GeM laboratory from March 1 2009 to June 26 2009 for the validation of the Master of Sciences in Computational Mechanics. At the end of this period, a BE formulation able to solve a potential problem was coded in C++, used to compute the displacement for a mode III problem in 2D and coupled to the propagation code.

Acknowledgements

This work was completed under the direction of N. Chevaugeon with the help of N. Moës, both teachers-researchers at ECN. I make a point of thanking them for the quality of their framing and the choice of the subject. I also express my admiration for their scientific and numeric competences, for the acuity of their analyses and the complementarity of their vision. I finally express to them all my gratitude as members of the team who animated the Erasmus Mundus master.

I thank the team of the GeM who ensures the network to be efficient and available. I am grateful to the authors of Gmsh, Mathematica and LaTeX to let us dispose of those powerful tools to carry out our work.

I thank my parents for their support, both material and affective. I also have a nice thought for all the people I met at ECN and GeM, specially Thibault, Céline, Raphaël, Corentin, Kristel, Kévin, Aurélie, Nicolas, Yvon, ...

List of Figures

Introduction

In this thesis, the boundary element method (BEM) is used for crack propagation. A BEM formulation is written to compute the elastic energy at any point required by the user, knowing the displacement or the traction on the boundary. Then it is coupled with a code of crack propagation using a level set technique which will use the former results to update the propagation criteria and determine new displacements and tractions on the boundary. Then those data and a mesh of the boundary (build from a level set) are sent to the BEM formulation (see fig.(1)). This loop stops when the crack does not propagate anymore.

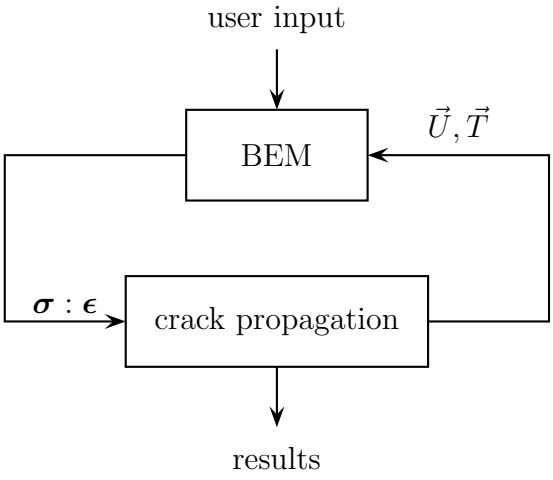

Figure 1: Schema of the interaction between BEM code and crack propagation code

In the first chapter, the elastostatic problem is presented and we show how the study of mode III leads to a potential problem. In the second chapter, the boundary element method is explicited for this problem with two formulations (use of constant or linear elements). A comparison of those formulations is illustrated with some test cases. In the third chapter, the crack propagation using a brittle damage law is detailled and we illustrate some results produced by the coupling of the two codes.

Chapter 1

Presentation of the problem

1.1 Notations

Quantities

We will write: a for a scalar quantity,
$\vec{a}$ for a vector,
$\mathbf{a}$ for a second order tensor (or higher order).

Operators

Gradient

In cartesian coordinates, the gradient of a is defined as:

$$\vec{\text{grad}}\ a(x,y,z) = (\frac{\partial a}{\partial x}, \frac{\partial a}{\partial y}, \frac{\partial a}{\partial z})$$

The vector $\vec{\text{grad}}\ a$ is also noted $\vec{\nabla} a$. The gradient operator creates a quantity one order higher than the argument.

Divergence

In cartesian coordinates, the gradient of $\vec{a} = (a_x, a_y, a_z)$ is defined as:

$$\text{div}\ \vec{a} = \frac{\partial a_x}{\partial x} + \frac{\partial a_y}{\partial y} + \frac{\partial a_z}{\partial z}$$

The scalar quantity div $\vec{a}$ is also noted $\vec{\nabla} \cdot \vec{a}$. The divergence operator creates a quantity one order lower than the argument. We will use the divergence of a product:

$$\vec{\nabla} \cdot (\lambda \vec{a}) = \lambda \vec{\nabla} \cdot \vec{a} + \vec{\nabla} \lambda \cdot \vec{a} \tag{1.1}$$

We will also need the Green-Ostrogradski theorem (divergence theorem):

$$\int_S \vec{\nabla} \cdot \vec{a} dS = \int_\Gamma \vec{a} \cdot d\vec{\Gamma} \tag{1.2}$$

Laplacian

The Laplacian operator is the composition of the divergence and the gradient. It is noted $\Delta = \vec{\nabla} \cdot \vec{\nabla}$ and creates a quantity of same order as the argument. In cartesian coordinates, the Laplacian of a is defined as:

$$\Delta a = \frac{\partial^2 a}{\partial x^2} + \frac{\partial^2 a}{\partial y^2} + \frac{\partial^2 a}{\partial z^2}$$

Normal derivative

$$\text{We note} \qquad \frac{\partial a}{\partial \vec{n}} = \vec{\nabla} a \cdot \vec{n}.$$

Norm

For a given vector $\vec{a}$ described by its components a_x and a_y in a two-dimensionnal basis, we note its norm:

$$\|\vec{a}\| = \sqrt{a_x^2 + a_y^2}$$

Dirac function

The Dirac function is defined by:

$$\begin{cases} \delta(\mathbf{y}, \mathbf{x}) = 0 & \text{if } \mathbf{y} \neq \mathbf{x} \\ \delta(\mathbf{y}, \mathbf{x}) = +\infty & \text{if } \mathbf{y} = \mathbf{x} \end{cases} \tag{1.3}$$

such that:

$$\forall \boldsymbol{\epsilon} \neq 0, \qquad \int_{\mathbf{x}-\boldsymbol{\epsilon}}^{\mathbf{x}+\epsilon} \delta(\mathbf{y}, \mathbf{x}) d\mathbf{y} = 1 \tag{1.4}$$

Kronecker index

The Kronecker index is defined by:

$$\begin{cases} \delta_{ij} = 0 & \text{if } i \neq j \\ \delta_{ij} = 1 & \text{if } i = j \end{cases}$$

Einstein convention

Considering $\mathcal{E}$ a vectorial space of dimension n, $(\mathbf{e}_1, \mathbf{e}_2, \ldots, \mathbf{e}_n)$ a random base of this space, and $\mathbf{V}$ a vector of $\mathcal{E}$, $\mathbf{V}$ can be written:

$$\mathbf{V} = \sum_{i=1}^{n} V^i \mathbf{e}_i$$

Einstein convention consists in omitting to write the sum on indices. Then the vector $\mathbf{V}$ is written:

$$\mathbf{V} = V^i \mathbf{e}_i$$

A sum index is a dummy index. It appears exactly twice in a monomial. As it is mute, its name has no meaning and can be replaced by another one:

$$\mathbf{V} = V^i \mathbf{e}_i = V^j \mathbf{e}_j$$

A real index (which is not mute) appears only once in a monomial and is the same in each monomial of an equation or a sum.

1.2 The elastostatic problem

The BEM will be applied to solve the following system:

$$\vec{div}(\boldsymbol{\sigma}) + \vec{f_v} = \vec{0} \tag{1.5}$$

$$\text{with} \begin{cases} \vec{u} = \vec{U} & \text{on } \Gamma_u \\ \vec{t} = \boldsymbol{\sigma}.\vec{n} = \vec{T} & \text{on } \Gamma_t \end{cases} \tag{1.6}$$

The behavior of the medium is described by:

$$\boldsymbol{\sigma} = 2\mu\boldsymbol{\epsilon} + \lambda tr(\boldsymbol{\epsilon})\mathbf{I} \tag{1.7}$$

The displacement field is written:

$$\epsilon_{ij} = \frac{1}{2}(u_{i,j} + u_{j,i}) \tag{1.8}$$

To ensure deformations to derive from such a displacement field, we use:

$$\boldsymbol{\Delta}(\boldsymbol{\epsilon}) + \mathbf{grad}(\vec{grad}(tr(\boldsymbol{\epsilon}))) = \mathbf{grad}(\vec{div}(\boldsymbol{\epsilon})) + \mathbf{grad}(\vec{div}(\boldsymbol{\epsilon}))^t \tag{1.9}$$

Using eq.(1.8) in eq.(1.7), we get:

$$\begin{aligned} \vec{div}(\boldsymbol{\sigma}) &= 2\mu\vec{div}(\boldsymbol{\epsilon}) + \lambda\vec{div}(tr(\boldsymbol{\epsilon})\mathbf{I}) \\ &= \mu\Big(\vec{div}(\mathbf{grad}\vec{u}) + \vec{div}(\mathbf{grad}\vec{u})^t\Big) + \lambda\Big(tr(\boldsymbol{\epsilon})\vec{div}(\mathbf{I}) + \mathbf{I}.\vec{grad}(tr(\boldsymbol{\epsilon}))\Big) \\ &= \mu\Big(\vec{\Delta}(\vec{u}) + \vec{div}(\mathbf{grad}(\vec{u})^t)\Big) + \lambda\vec{grad}(div(\vec{u})) \\ &= \mu\vec{\Delta}(\vec{u}) + (\lambda+\mu)\vec{grad}(div(\vec{u})) \end{aligned}$$

Putting this expression in the equilibrium equation yields the Lamé-Clapeyron equation:

$$\mu\vec{\Delta}(\vec{u}) + (\lambda+\mu)\vec{grad}(div(\vec{u})) + \vec{f_v} = \vec{0} \tag{1.10}$$

Mode III problem

In this thesis, we focused on solving the mode III problem. Indeed, the elstostatic problem can be written as a potential problem, which is simpler to treat (as shown in [2]). The final objective is to have a boundary element formulation able to solve the general elastostatic problem, but due to a matter of time, this work could not be achieved. To implement it, the basis can be found in [3].

For in-plane problems, we can write the Papkovich representation for the displacement field:

$$2\mu\vec{u} = 4(1-\nu)\vec{\psi} - grad(\phi + \vec{r}\cdot\vec{\psi}) \tag{1.11}$$

where in the unit orthogonal basis $(\vec{e_x}, \vec{e_y}, \vec{e_z})$, $\vec{u} = u_x\vec{e_x} + u_y\vec{e_y} + u_z\vec{e_z}$ is the displacement vector, $\vec{r} = r_x\vec{e_x} + r_y\vec{e_y} + r_z\vec{e_z}$ is the position vector and ϕ and $\vec{\psi} = \psi_x\vec{e_x} + \psi_y\vec{e_y} + \psi_z\vec{e_z}$ are scalar and vector potentials which satisfy the equations:

$$\Delta\phi = 0 \qquad \vec{\Delta}\vec{\psi} = \vec{0} \tag{1.12}$$

Insertion shows that the Papkovich representation satisfies the equations of equilibrium after putting the inertia term equal to zero. As shown by Eubanks and Sternberg [7], one of the four potential function may be put to zero under rather general conditions. Specialization to plane strain, $u_x = u_x(x,y), u_y = u_y(x,y), u_z = 0$, implies that the potentials are function of x and y, only, and then, according to 1.11:

$$\psi_z = 0 \tag{1.13}$$

It remains only the scalar variables ϕ, ψ_x and ψ_y. As they are independant, we search only the solution of $\Delta u = 0$ where the unknown u is a scalar (see chapter 2).

An analytical solution has been given for the steady-state problem of the dynamic propagation of a damaged zone in elastic body, in permanent mode III [4]. The shape of the propagation front was computed to be a cycloid with a cusp.

Other assumptions leading to a potential problem

Note that this potential problem could also be considered as the elastostatic problem under simplifying assumptions. Indeed we get a potential problem in a case of pure deformation (no rotation of solid body) without any body forces. Thanks to the pure deformation assumption, the displacement field derives from a potential ϕ: $\vec{u} = \vec{grad}(\phi)$. Then Lamé-Clapeyron equations (1.10) become:

$$(\lambda+2\mu)\vec{\Delta}(\vec{u}) + \vec{f_v} = \vec{0} \tag{1.14}$$

And without body forces, we get the harmonic function:

$$\vec{\Delta}(\vec{u}) = \vec{0} \tag{1.15}$$

Let us remark that we also come to the same result assuming that the medium is incompressible. Indeed, then we have $tr(\boldsymbol{\epsilon}) = div(\vec{u}) = 0$ so eq.(1.10) become:

$$\mu\vec{\Delta}(\vec{u}) + \vec{f_v} = \vec{0} \tag{1.16}$$

And without body forces, we find back eq.(1.15).

As this equation can be written independantly for each component of $\vec{u}$, we study the following problem on the scalar unknown u.

Boundary conditions

We note $\vec{v}$ the flux related to u computed anywhere on the domain S:

$$\vec{v}(\vec{x}) = \vec{\nabla} u(\vec{x}) \tag{1.17}$$

and v the scalar normal flux computed anywhere on the boundary Γ:

$$v(\vec{x}) = \frac{\partial u(\vec{x})}{\partial \vec{n^e}(\vec{x})} \tag{1.18}$$

where $\vec{n^e}(\vec{x})$ is the outside unit normal vector to the boundary at point $\vec{x}$.

The potential problem for the scalar unknown u is written for the following boundary conditions:

$$\left\{ \begin{array}{ll} \Delta u(\vec{x}) = 0 & \forall \vec{x} \in S \\ u(\vec{x}) = \bar{u}(\vec{x}) & \forall \vec{x} \in \Gamma_u \\ v(\vec{x}) = \bar{v}(\vec{x}) & \forall \vec{x} \in \Gamma_v \end{array} \right. \tag{1.19}$$

Γ_u	:	part of the boundary with prescribed Dirichlet conditions
$\bar{u}$	:	prescribed Dirichlet conditions
Γ_v	:	part of the boundary with prescribed Newman conditions
$\bar{v}$	:	prescribed Newman conditions

where $\{\Gamma_u, \Gamma_v\}$ constitutes a partition of Γ, that is:

$$\begin{array}{rcl} \Gamma_u \cup \Gamma_v & = & \Gamma \\ \Gamma_u \cap \Gamma_v & = & \emptyset \end{array}$$

Chapter 2

Potential problem

In this chapter, we expose how the BEM can solve the problem (1.19).

The BEM is a numerical technique developed since the early sixties and founded on the older theory of Boundary Integral Equation (BIE). This theory appeared in the nineteenth century throught the work of Poisson (1820), Betty (1872), Kirchhoff (1882), Fredholm (1896), Kellog (1929), Kupradze (1935). Then in the sixties, Jaswon [12], Hess [11], Symm, Shaw, Rizzo, Cruse and others worked on the BEM (the name BEM appeared only in 1977). In particular, Frank J Rizzo [18] was one of the pionner of a novel direct boundary integral method for the numerical solution of elasticity problems. Since then, many papers have been written on this method and it is still an active theme of research in various fields such as cracks and heat diffusion [1], acoustic [6], meteorology [17] or reflection seismology [5] [15].

This method represents an alternative to another numerical method: the finite element method (FEM). The main advantage of BEM is to deal very well with infinite media, and also to require only a mesh on the boundary, not inside the domain. However, the details of the computation with FEM are easier to interpret and once the formulation is written, it produces sparse matrices (instead of dense ones for BEM).

Most of the following work has been done thanks to [3] and [13].

2.1 BEM formulation

2.1.1 Transformation of the problem

As in many methods, we cancel the average error on the main equation using a weighing function w. That is we ensure:

$$\int_S \Delta u \omega dS = 0 \tag{2.1}$$

We note:

$$\omega = u^* \qquad \text{and} \qquad \frac{\partial \omega}{\partial \vec{n^e}} = v^* \tag{2.2}$$

Now we apply some mathematical transformations to eq.(2.1) in order to introduce the boundary fields. The formula of the divergence of a product eq.(1.1) yields:

$$\vec{\nabla} \cdot (u^* \vec{\nabla} u) = u^* \vec{\nabla} \cdot \vec{\nabla} u + \vec{\nabla} u^* \cdot \vec{\nabla} u$$

Then taking the integral over the domain S, we can write:

$$\int_S u^* \Delta u dS = \int_S \vec{\nabla} \cdot (u^* \vec{\nabla} u) dS - \int_S \vec{\nabla} u^* \cdot \vec{\nabla} u dS \tag{2.3}$$

And the Green-Ostrogradski theorem eq.(1.2) gives:

$$\int_S \vec{\nabla} \cdot (u^* \vec{\nabla} u) dS = \int_\Gamma u^* \vec{\nabla} u \cdot d\vec{\Gamma} \tag{2.4}$$

We introduce $\vec{n^e}$ the normal vector to Γ pointing outward. As $v = \vec{\nabla} u \cdot \vec{n^e}$, we can write:

$$\int_\Gamma u^* \vec{\nabla} u \cdot d\vec{\Gamma} = \int_\Gamma u^* \vec{\nabla} u \cdot \vec{n^e} d\Gamma = \int_\Gamma u^* v d\Gamma \tag{2.5}$$

So we get from equations (2.3), (2.4) and (2.5):

$$\int_S u^* \Delta u dS = \int_\Gamma u^* v d\Gamma - \int_S \vec{\nabla} u^* \cdot \vec{\nabla} u dS \tag{2.6}$$

Then we repeat the same computation steps on the last integral and obtain:

$$\int_S \vec{\nabla} u^* \cdot \vec{\nabla} u dS = \int_\Gamma u v^* d\Gamma - \int_S u \Delta u^* dS$$

So we can write:

$$\int_S u^* \Delta u dS = \int_\Gamma u^* v d\Gamma - \int_\Gamma u v^* d\Gamma + \int_S u \Delta u^* dS \tag{2.7}$$

And the main equation (2.1) becomes:

$$\int_\Gamma u^* v d\Gamma - \int_\Gamma u v^* d\Gamma + \int_S u \Delta u^* dS = 0 \tag{2.8}$$

2.1.2 Fundamental solution

Let us remind that eq.(2.8) has been written for any weighing function u^*. Now we choose for u^* the solution corresponding to a source located at $\vec{y}$ inside the domain Ω:

$$\forall \vec{x} \in \Omega, \qquad \forall \vec{y} \in \Omega \backslash \Gamma, \qquad \Delta u^*(\vec{x}, \vec{y}) = -\delta(\vec{x}, \vec{y}) \tag{2.9}$$

u^* is called the fundamental solution, $\vec{y}$, the source point and $\vec{x}$, the potented point. This particular choice of u^* will allow us to compute easily the integral on Ω in eq.(2.8).

Noting $r = \|\vec{x} - \vec{y}\|$, we explicit the fundamental solution of eq.(2.9) u^* and its normal derivative v^* for an isotropic two or three dimensionnal medium:

$2D$ (cylindrical coordinates)		$3D$ (spherical coordinates)	
$u^*(r)$	$= \frac{1}{2\pi} ln(\frac{1}{r})$	$u^*(r)$	$= \frac{1}{4\pi r}$
$v^*(\vec{y},\vec{x})$	$= (\frac{\partial u^*}{\partial r}\vec{e_r} + \frac{1}{r}\frac{\partial u^*}{\partial \theta}\vec{e_\theta} + \frac{\partial u^*}{\partial z}\vec{e_z}).\vec{n^e}$	$v^*(\vec{y},\vec{x})$	$= (\frac{\partial u^*}{\partial r}\vec{e_r} + \frac{1}{r}\frac{\partial u^*}{\partial \theta}\vec{e_\theta} + \frac{1}{rsin(\theta)}\frac{\partial u^*}{\partial \phi}\vec{e_\phi}).\vec{n^e}$
	$= (\frac{\partial u^*}{\partial r}\vec{e_r}).\vec{n^e}$		$= (\frac{\partial u^*}{\partial r}\vec{e_r}).\vec{n^e}$
	$= -\frac{1}{2\pi r}\vec{e_r}.\vec{n^e}$		$= -\frac{1}{4\pi r^2}\vec{e_r}.\vec{n^e}$

where $\vec{e_r} = \frac{\vec{y}-\vec{x}}{\|\vec{y}-\vec{x}\|}$ and $\vec{n^e} = \vec{n^e}(\vec{x})$.

2.1.3 Computation of the fields and fluxes

When we put the fundamental solution u^* into eq.(2.8), the Dirac property eq.(1.4) yields:

$$\forall \vec{y} \in \Omega\backslash\Gamma, \qquad u(\vec{y}) = \int_\Gamma v(\vec{x})u^*(\vec{y},\vec{x})d\Gamma(\vec{x}) - \int_\Gamma u(\vec{x})v^*(\vec{y},\vec{x})d\Gamma(\vec{x}) \tag{2.10}$$

Using this equation in the definition of the flux $\vec{v}$ (see eq.(1.17)), we get:

$$\forall \vec{y} \in \Omega\backslash\Gamma, \qquad \vec{v}(\vec{y}) = \int_\Gamma v(\vec{x})\vec{\nabla}_{\vec{y}}(u^*(\vec{y},\vec{x}))d\Gamma(\vec{x}) - \int_\Gamma u(\vec{x})\vec{\nabla}_{\vec{y}}(v^*(\vec{y},\vec{x}))d\Gamma(\vec{x}) \tag{2.11}$$

where $\vec{\nabla}_{\vec{y}}$ indicates that the gradient is taken relatively to $\vec{y}$.

For a source point $\vec{x}'$ located on the boundary Γ, eq.(2.10) is slightly different. Indeed, as the distance r between $\vec{x}'$ and the point $\vec{x}$ describing Γ can cancel, singularities appear in the integrals. Let Γ_ϵ be a circular boundary curve of center $\vec{x}'$ and radius ϵ as illustrated in fig.(2.1) for $\epsilon = 1$. Since we have:

$$\Gamma = \lim_{\epsilon\to 0}(\Gamma\backslash\Gamma_\epsilon) \cup \Gamma_\epsilon$$

we can write from eq.(2.10):

$$\begin{aligned} u(\vec{x}') &= \lim_{\epsilon\to 0}\Big[\int_{\Gamma_\epsilon} v(\vec{x})u^*(\vec{x}',\vec{x})d\Gamma(\vec{x}) - \int_{\Gamma_\epsilon} u(\vec{x})v^*(\vec{x}',\vec{x})d\Gamma(\vec{x}) && (2.12)\\ &\quad + \int_{\Gamma\backslash\Gamma_\epsilon} v(\vec{x})u^*(\vec{x}',\vec{x})d\Gamma(\vec{x}) - \int_{\Gamma\backslash\Gamma_\epsilon} u(\vec{x})v^*(\vec{x}',\vec{x})d\Gamma(\vec{x})\Big] && (2.13)\end{aligned}$$

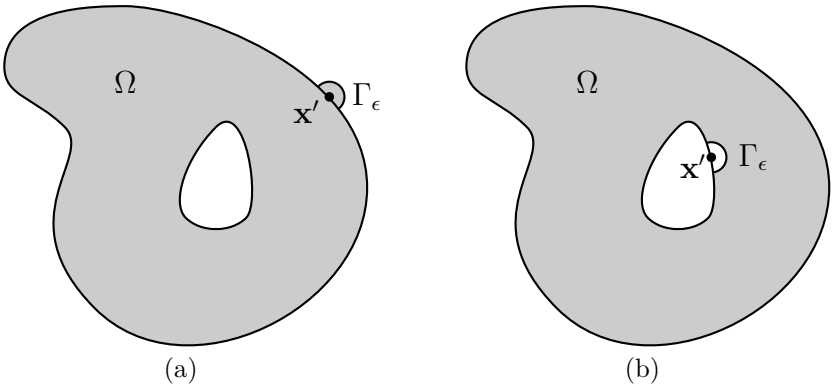

Figure 2.1: Γ_ϵ for a given $\mathbf{x}'$ on the outer (a) or inner (b) boundary (2D problem)

Now the singularities are isolated in integrals on Γ_ϵ. Assuming that the boundary is smooth at $\vec{x}'$ (i.e. $\vec{x}'$ is a regular point), Γ_ϵ tends to be a half-circle when ϵ tends to zero. So we compute:

$$\begin{aligned}\lim_{\epsilon\to 0}\int_{\Gamma_\epsilon} v(\vec{x})u^*(\vec{x}',\vec{x})d\Gamma(\vec{x}) &= \lim_{\epsilon\to 0}\int_{\Gamma_\epsilon} v(\vec{x})\frac{1}{2\pi}ln(\frac{1}{\epsilon})d\Gamma(\vec{x}) \\ &= \lim_{\epsilon\to 0} v(\vec{x}')\frac{\pi\epsilon}{2\pi}ln(\frac{1}{\epsilon}) \\ &= 0\end{aligned}$$

$$\lim_{\epsilon\to 0} -\int_{\Gamma_\epsilon} u(\vec{x})v^*(\vec{x}',\vec{x})d\Gamma(\vec{x}) = \lim_{\epsilon\to 0}\int_{\Gamma_\epsilon} u(\vec{x})\frac{1}{2\pi\epsilon}\vec{e_r}.\vec{n^e}d\Gamma(\vec{x})$$

We define the function σ for each point $\vec{x}'$ of the boundary Γ such that:

$$\sigma(\vec{x}') = \begin{cases} +1 & \text{if } \vec{x}' \text{ is on an outer boundary} \\ -1 & \text{if } \vec{x}' \text{ is on an inner boundary} \end{cases} \tag{2.14}$$

Then we have $\sigma(\vec{x}') = \vec{e_r}(\vec{x},\vec{x}').\vec{n^e}(\vec{x})$ as illustrated in fig.(2.2).

$$\begin{aligned}\lim_{\epsilon\to 0} -\int_{\Gamma_\epsilon} u(\vec{x})v^*(\vec{x}',\vec{x})d\Gamma(\vec{x}) &= \lim_{\epsilon\to 0} u(\vec{x}')\frac{\pi\epsilon}{2\pi\epsilon}\sigma(\vec{x}') \\ &= \frac{1}{2}u(\vec{x}')\sigma(\vec{x}')\end{aligned}$$

so they produce a free term.

Now, let us assume that the boundary is not smooth at $\vec{x}'$ but describes a corner (i.e. $\vec{x}'$ is a singular point). Then Γ_ϵ tends to be an arc of circle of angle $\theta(\vec{x}')$ when ϵ tends to zero, as illustrated in fig.(2.3).

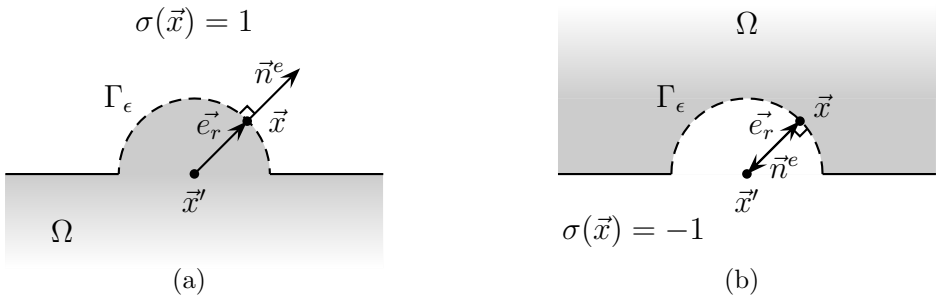

Figure 2.2: Different values of $\sigma(\vec{x})$ for $\vec{x}$ on the outer (a) or inner (b) boundary

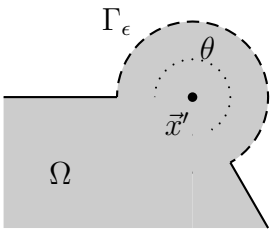

Figure 2.3: Γ_ϵ at a convexe corner $\mathbf{x}'$ on a outer boundary ($\theta(\mathbf{x}') > \pi$)

So we get:

$$\begin{aligned}\lim_{\epsilon\to 0}\int_{\Gamma_\epsilon} v(\vec{x})u^*(\vec{x}',\vec{x})d\Gamma(\vec{x}) &= \lim_{\epsilon\to 0}\int_{\Gamma_\epsilon} v(\vec{x})\frac{1}{2\pi}ln(\frac{1}{\epsilon})d\Gamma(\vec{x}) \\ &= \lim_{\epsilon\to 0} v(\vec{x}')\frac{\theta(\vec{x}')}{2\pi}ln(\frac{1}{\epsilon}) \\ &= 0\end{aligned}$$

$$\begin{aligned}\lim_{\epsilon\to 0} -\int_{\Gamma_\epsilon} u(\vec{x})v^*(\vec{x}',\vec{x})d\Gamma(\vec{x}) &= \lim_{\epsilon\to 0}\int_{\Gamma_\epsilon} u(\vec{x})\frac{1}{2\pi\epsilon}\vec{e_r}.\vec{n^e}d\Gamma(\vec{x}) \\ &= \lim_{\epsilon\to 0} u(\vec{x}')\frac{\theta(\vec{x}')}{2\pi\epsilon}\sigma(\vec{x}') \\ &= \frac{\theta(\vec{x}')}{2\pi}u(\vec{x}')\sigma(\vec{x}')\end{aligned}$$

Of course, we find back the case of a smooth boundary when $\theta(\vec{x}') = \pi$.

The two other integrals of eq.(2.12) are not affected when ϵ tends to 0 because singularities are located on Γ_ϵ only. So we get:

$$(1 - \frac{\theta(\vec{x}')}{2\pi}\sigma(\vec{x}'))u(\vec{x}') = \int_\Gamma v(\vec{x})u^*(\vec{x}',\vec{x})d\Gamma(\vec{x}) - \int_\Gamma u(\vec{x})v^*(\vec{x}',\vec{x})d\Gamma(\vec{x}) \qquad (2.15)$$

With eq.(2.15), we can compute the field u and its derivative v anywhere on the boundary. Once this is done, we will use eq.(2.10) and eq.(2.11) to compute respectively the field u and the flux $\vec{v}$ anywhere inside the domain. To evaluate those integrals, we discretize the boundary and ensure the boundary conditions only at nodes, which allows to transform integrals into finite sums. In the following sections, we will present two different discretizations of the boundary: the first one using constant elements (section 2.2) and the second one using linear elements (section 2.3).

2.2 Computation using constant elements

2.2.1 Discretization of the boundary

We approximate the boundary Γ with N segments Γ_j (where $j = 1, \ldots, N$) carrying constant fields u_j and v_j. The nodes are located at their middle point $\vec{x}_j$ (see fig.(2.4)). Due to this choice, we always are in the case of a smooth boundary: $\frac{\theta_i}{2\pi} = \frac{1}{2}$.

Now the constant values u_j and v_j can be taken out of the integrals of eq.(2.15) so that we obtain for any $\vec{x}'$ on Γ:

$$(1 - \frac{1}{2}\sigma(\vec{x}'))u(\vec{x}') = \sum_{j=1}^{N} \Big(\int_{\Gamma_j} u^*(\vec{x}', \vec{x}) d\Gamma(\vec{x}) \Big) v_j - \sum_{j=1}^{N} \Big(\int_{\Gamma_j} v^*(\vec{x}', \vec{x}) d\Gamma(\vec{x}) \Big) u_j \qquad (2.16)$$

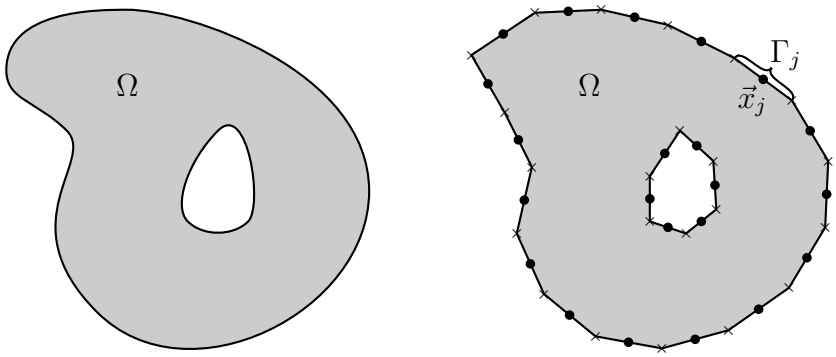

Figure 2.4: Discretization of a geometry (a) with constant elements (b).

Let us work at a given i in $(1, \ldots, N)$. Noting $\theta_i = \theta(\vec{x}_i)$ and $\sigma_i = \sigma(\vec{x}_i)$, we get :

$$(1 - \frac{\sigma_i}{2})u_i = \sum_{j=1}^{N} \Big(\int_{\Gamma_j} u^*(\vec{x}_i, \vec{x}) d\Gamma(\vec{x}) \Big) v_j - \sum_{j=1}^{N} \Big(\int_{\Gamma_j} v^*(\vec{x}_i, \vec{x}) d\Gamma(\vec{x}) \Big) u_j \qquad (2.17)$$

$$\text{We define} \qquad G_{ij} = \int_{\Gamma_j} u^*(\vec{x}_i, \vec{x}) d\Gamma(\vec{x}) \qquad \text{and} \qquad H_{ij} = \int_{\Gamma_j} v^*(\vec{x}_i, \vec{x}) d\Gamma(\vec{x})$$

G_{ij} and H_{ij} are explicited in appendix (A).

$$\begin{aligned} \text{Then,} \qquad (1 - \frac{\theta_i}{2\pi}\sigma_i)u_i &= \sum_{j=1}^{N} G_{ij}v_j - \sum_{j=1}^{N} H_{ij}u_j \\ &= \sum_{j/(\Gamma_j \subset \Gamma_1)} \Big(G_{ij}v_j - H_{ij}\bar{u}_j \Big) + \sum_{j/(\Gamma_j \subset \Gamma_2)} \Big(G_{ij}\bar{v}_j - H_{ij}u_j \Big) \end{aligned}$$

$$\text{Let us note} \qquad \widetilde{H}_{ij} = H_{ij} + (1 - \frac{\sigma_i}{2})\delta_{ij}$$

$$\text{If } \Gamma_i \subset \Gamma_1, \qquad \sum_{j/(\Gamma_j \subset \Gamma_1)} G_{ij}v_j - \sum_{j/(\Gamma_j \subset \Gamma_2)} H_{ij}u_j = \sum_{j/(\Gamma_j \subset \Gamma_1)} \widetilde{H}_{ij}\bar{u}_j - \sum_{j/(\Gamma_j \subset \Gamma_2)} G_{ij}\bar{v}_j$$

$$\text{If } \Gamma_i \subset \Gamma_2, \qquad \sum_{j/(\Gamma_j \subset \Gamma_1)} G_{ij}v_j - \sum_{j/(\Gamma_j \subset \Gamma_2)} \widetilde{H}_{ij}u_j = \sum_{j/(\Gamma_j \subset \Gamma_1)} H_{ij}\bar{u}_j - \sum_{j/(\Gamma_j \subset \Gamma_2)} G_{ij}\bar{v}_j$$

So we can write the following system:

$$\begin{pmatrix} -G_{ik} & H_{il} \\ -G_{ik} & \widetilde{H}_{il} \end{pmatrix} \begin{pmatrix} v_k \\ u_l \end{pmatrix} = \begin{pmatrix} -\widetilde{H}_{ik} & G_{il} \\ -H_{ik} & G_{il} \end{pmatrix} \begin{pmatrix} \bar{u}_k \\ \bar{v}_l \end{pmatrix} \qquad \text{where} \begin{cases} k \text{ such that } \Gamma_k \subset \Gamma_1 \\ l \text{ such that } \Gamma_l \subset \Gamma_2 \end{cases} \tag{2.18}$$

This can be seen as a system of the form:

$$\mathbf{Ax} = \mathbf{b}$$

where $\mathbf{x}$ is the vector of unknowns at the nodes while $\mathbf{A}$ and $\mathbf{b}$ gather information on the geometry and the boundary conditions. So once the system (2.18) is solved, the field u and the flux v are known at any point of the boundary.

2.2.2 Computation of the fields anywhere

Knowing the fields u and v anywhere on the boundary, we can compute the field u anywhere inside the domain thanks to eq.(2.10). After discretization, the constant values u_j and v_j on Γ_j can be taken out the integrals again:

$$\forall \vec{y} \in \Omega, \qquad u(\vec{y}) = \sum_{j=1}^{N} \Big(\int_{\Gamma_j} u^*(\vec{y}, \vec{x}) d\Gamma(\vec{x}) \Big) v_j - \sum_{j=1}^{N} \Big(\int_{\Gamma_j} v^*(\vec{y}, \vec{x}) d\Gamma(\vec{x}) \Big) u_j \tag{2.19}$$

$$\text{We note} \qquad G_j(\vec{y}) = \int_{\Gamma_j} u^*(\vec{y}, \vec{x}) d\Gamma(\vec{x}) \qquad \text{and} \qquad H_j(\vec{y}) = \int_{\Gamma_j} v^*(\vec{y}, \vec{x}) d\Gamma(\vec{x}) \tag{2.20}$$

Since $G_{ij} = G_j(\vec{x}_i)$ and $H_{ij} = H_j(\vec{x}_i)$, we will compute them with the formulae given in appendix (A).

2.2.3 Computation of the fluxes anywhere

Knowing the fields u and v anywhere on the boundary, we can compute the flux $\vec{v}$ anywhere inside the domain thanks to eq.(2.11). After discretization, the constant values u_j and v_j on Γ_j can be taken out the integrals again:

$$\forall \vec{y} \in \Omega, \qquad \vec{v}(\vec{y}) = \sum_{j=1}^{N} \Big(\int_{\Gamma_j} \vec{\nabla}_{\vec{y}}(u^*(\vec{y},\vec{x}))d\Gamma(\vec{x}) \Big) v_j - \sum_{j=1}^{N} \Big(\int_{\Gamma_j} \vec{\nabla}_{\vec{y}}(v^*(\vec{y},\vec{x}))d\Gamma(\vec{x}) \Big) u_j \tag{2.21}$$

$$\text{We define} \qquad G_j^v(\vec{y}) = \int_{\Gamma_j} \vec{\nabla}_{\vec{y}}(u^*(\vec{y},\vec{x}))d\Gamma(\vec{x}) \qquad \text{and} \qquad H_j^v(\vec{y}) = \int_{\Gamma_j} \vec{\nabla}_{\vec{y}}(v^*(\vec{y},\vec{x}))d\Gamma(\vec{x}) \tag{2.22}$$

so that we can write:

$$\forall \vec{y} \in \Omega, \qquad \vec{v}(\vec{y}) = \sum_{j=1}^{N} G_j^v(\vec{y}) v_j - \sum_{j=1}^{N} H_j^v(\vec{y}) u_j \tag{2.23}$$

Due to a lack of time, the correct analytic formulae of G_{ij}^v and H_{ij}^v have not been written. Consequently, in the code the fluxes are computed using a finite difference. For dx and dy small enough, we compute:

$$\forall \vec{y} \in \Omega, \qquad v_x(\vec{y}) \approx \frac{u(\vec{y} + dx\vec{e}_x) - u(\vec{y})}{dx} \qquad \text{and} \qquad v_y(\vec{y}) \approx \frac{u(\vec{y} + dy\vec{e}_y) - u(\vec{y})}{dy} \tag{2.24}$$

A special care is taken to choose the size and the sign of dx and dy in order that $\vec{y} + dx\vec{e}_x$ and $\vec{y} + dy\vec{e}_y$ stay inside the domain.

2.2.4 Computation of matrices for BEM

$$G_{ij} = \int_{\Gamma_j} \frac{1}{2\pi} ln(\frac{1}{r}) d\Gamma(\vec{x}) \qquad \text{and} \qquad H_{ij} = \int_{\Gamma_j} -\frac{1}{2\pi r} \vec{e_r}.\vec{n} d\Gamma(\vec{x}) \tag{2.25}$$

$$\text{where} \qquad r = \|\vec{x} - \vec{x}_i\| \tag{2.26}$$

Let us remind that $\vec{x}$ is the point which describes the boundary element Γ_j and $\vec{x}_i$ is the middle point of the boundary element Γ_i. We note $\vec{p_1}^i$ and $\vec{p_2}^i$ the points of the extremity of element Γ_i, and $x_1^i, y_1^i, x_2^i, y_2^i$ their respective components in an orthonormal two-dimensionnal basis (see fig.(2.5)). Since boundary elements are linear geometries (i.e. segments), we have:

$$\vec{x} \in \Gamma_j \qquad \Leftrightarrow \qquad \exists s \in [0,1], \vec{x} = \vec{p_1}^j + s(\vec{p_2}^j - \vec{p_1}^j) \tag{2.27}$$

The middle point is the average of the two extremities of the related segment, so we get: $\vec{x}_i = \frac{\vec{p_1}^i + \vec{p_2}^i}{2}$.

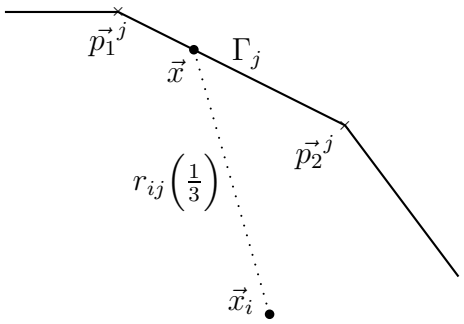

Figure 2.5: The distance r for s=1/3

This yields:

$$\begin{aligned} r_{ij} &= \|\vec{p_1}^j + s(\vec{p_2}^j - \vec{p_1}^j) - \frac{\vec{p_1}^i + \vec{p_2}^i}{2}\| \\ &= \sqrt{\left(x_1^j + s(x_2^j - x_1^j) - \frac{x_1^i + x_2^i}{2})\right)^2 + \left(y_1^j + s(y_2^j - y_1^j) - \frac{y_1^i + y_2^i}{2}\right)^2} \\ &= \sqrt{\alpha_{ij} + \beta_{ij} s + \gamma_{ij} s^2} \end{aligned}$$

where
$$\begin{cases} \alpha_{ij} &= \left(x_1^j - \frac{x_1^i + x_2^i}{2}\right)^2 + \left(y_1^j - \frac{y_1^i + y_2^i}{2}\right)^2 = \|\overrightarrow{p_1^j p_i}\|^2 \\ \beta_{ij} &= 2\Big((x_1^j - \frac{x_1^i + x_2^i}{2})(x_2^j - x_1^j) + (y_1^j - \frac{y_1^i + y_2^i}{2})(y_2^j - y_1^j)\Big) = 2\overrightarrow{p_i p_1^j} \cdot \overrightarrow{p_1^j p_2^j} \\ \gamma_{ij} &= (x_2^j - x_1^j)^2 + (y_2^j - y_1^j)^2 = \|\overrightarrow{p_1^j p_2^j}\|^2 = |\Gamma_j|^2 \end{cases}$$

Since $d\Gamma_j = \sqrt{\gamma_{ij}} ds$ we can write:

$$G_{ij} = \int_0^1 -\frac{ln(\alpha_{ij} + \beta_{ij} s + \gamma_{ij} s^2)}{4\pi} \sqrt{\gamma_{ij}} ds \qquad \text{and} \qquad H_{ij} = \int_0^1 -\frac{\sqrt{\gamma_{ij}}}{2\pi\sqrt{\alpha_{ij} + \beta_{ij} s + \gamma_{ij} s^2}} ds$$

In the following, we will allow us to forget the indices i and j. Now that all quantities of eq.(2.25) are expressed with respect to the coordinates of $\vec{x}_i$ and $\vec{x}_j$, we can compute explicitly[1] G_{ij} and H_{ij}. They are continuously defined but their litteral expression depends on the sign of the determinant $D = \beta^2 - 4\alpha\gamma$ of the second order polynom $r_{ij}^2(s)$:

[1]The full computation of G_{ij} and H_{ij} is detailled in sections A.2 and A.3 respectively.

If $D < 0$, then we have:

$$\begin{aligned} G_{ij} &= -\frac{\sqrt{\gamma}}{4\pi}\Big[\Big(1+\frac{\beta}{2\gamma}\Big)ln(|\alpha+\beta+\gamma|) - \frac{\beta}{2\gamma}ln(\alpha) - 2 \\ &\quad + \frac{\sqrt{-D}}{\gamma}\Big(arctan\Big(\frac{\beta+2\gamma}{\sqrt{-D}}\Big) - arctan\Big(\frac{\beta}{\sqrt{-D}}\Big)\Big)\Big] \\ H_{ij} &= -\frac{\sigma_j\sqrt{\gamma}}{2\pi}\Big(arctan\Big(\frac{\beta+2\gamma}{\sqrt{-D}}\Big) - arctan\Big(\frac{\beta}{\sqrt{-D}}\Big)\Big) \end{aligned}$$

If $D = 0$, then we have:

$$\begin{aligned} G_{ij} &= -\frac{\sqrt{\gamma}}{4\pi}\Big[ln(|\alpha+\beta+\gamma|) - 2 + \frac{\beta}{\gamma}ln\Big(\Big|\frac{2\gamma}{\beta}+1\Big|\Big)\Big] \\ H_{ij} &= 0 \end{aligned}$$

Let us remark that in the case where $D = 0$, as $\beta^2 = 4\alpha\gamma$ and α and γ are strictly positive, β cannot cancel. So the logarithm used in G and H is well-defined.

2.2.5 Test cases

In order to evaluate the accuracy of the solution computed with the BEM, we only work with simple cases for which we know the analytical solution in this section. So we work on only two kinds of two-dimensionnal problems: cases equivalent to one-dimensionnal problems (with revolution symmetry or invariance in one direction) and cases with decouplable variables (as a rectangle space).

Each test is illustrated with a couple of figures showing respectively the displacement and the flux vector. The size is sized from the miniumum to the maximum of the values (or norm of vectors) which are reached.

Crown problem

We run the case of a crown for which we impose Dirichlet boundary conditions: $u = 0$ everywhere on the inner circle and $u = 1$ everywhere on the outer circle. The analytical field is linear towards the distance to the center of the crown (see appendix D).

The formulation requires that all the nodes of the domain mesh are inside the area delimited by the boundary mesh. As the elements are described by segments, the boundary mesh cannot describe exactly a circle, but approximates it by a polygon. So when treating with a curvature, the domain mesh should be confounded with the boundary mesh on the boundaries, or always remain slightly inside the area delimited by the boundary mesh. For the study of the crown, we choosed to change the geometry used for the domain mesh to avoid this problem. That is why on fig.(2.6), u never reachs the boundary conditions (look at the scale) although they are exactly satisfied.

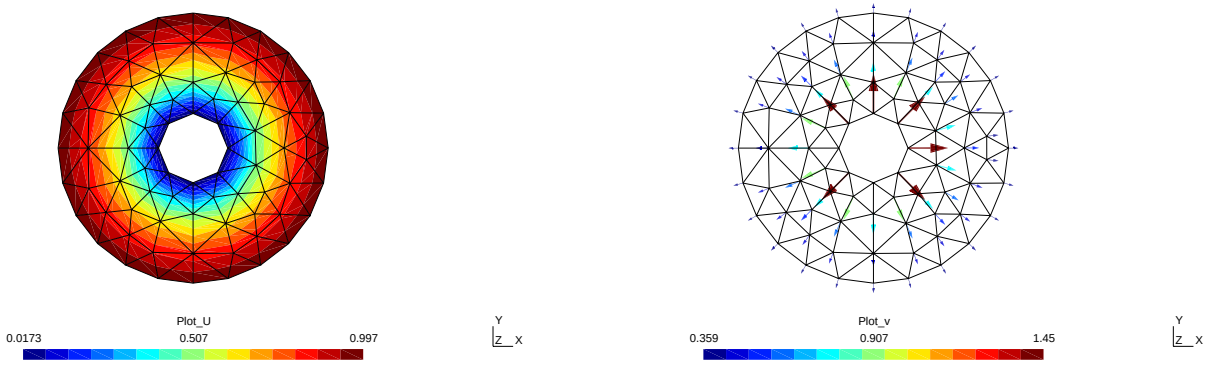

Figure 2.6: Field and flux on a crown computed with constant elements

We have launched the computation on the crown problem with four different meshes:

caracteristic length	number of dof	time				precision of the results
		fill matrices	solve the system	evaluate inside	total	
0.05	308	0.11s	0.04s	0.04s	0.21s	[-7;-10]
0.02	784	1.09s	1.47s	0.10s	2.72s	[-8.5;-12]
0.015	1044	2.18s	5.38s	0.13s	7.78s	[-9;-13]
0.01	1568	5.37s	21.93s	0.29s	27.75s	[-10;-15]
0.005	3140	25.77s	185.44s	0.74s	213.31s	[-6.5;-10]

With BEM, the number of degrees of freedom (dof) handled in the system is the number of nodes of the boundary mesh, whereas FEM requires the use of dof distributed everwhere in the domain. So the BEM deals with one dimension less unknowns than the FEM. That is why those computational times are much lower than what could do the FEM for an equivalent problem (same boundary conditions and caracteristic length).

We can see on figure (2.9) that the time needed to evaluate the field in a point inside the domain is linearly proportionnal to the number of nodes on the boundary.

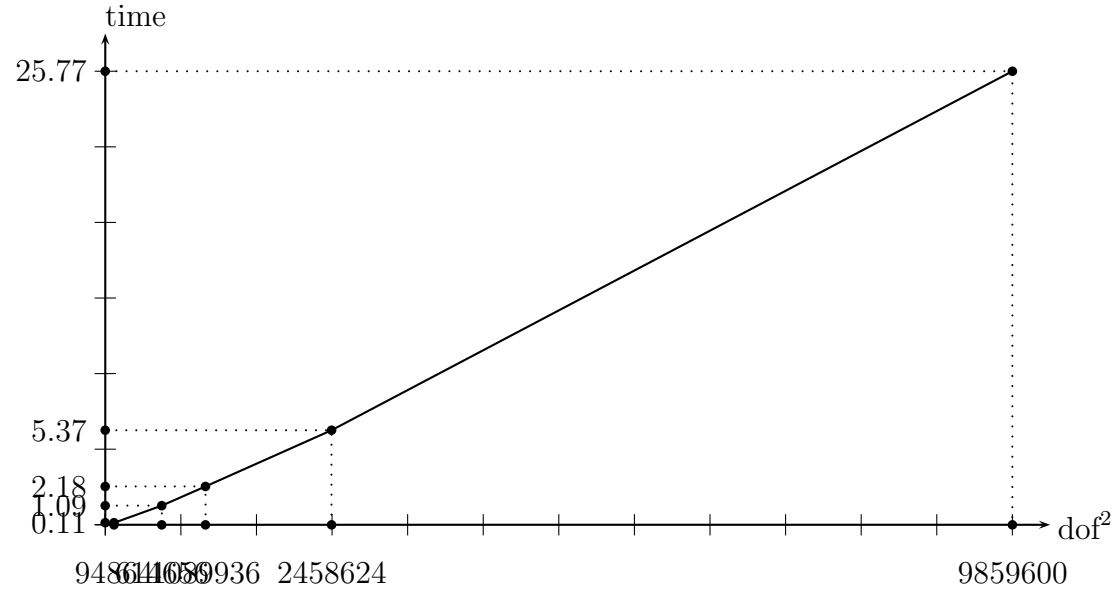

Figure 2.7: Relation between time needed to fill the matrices and dof.

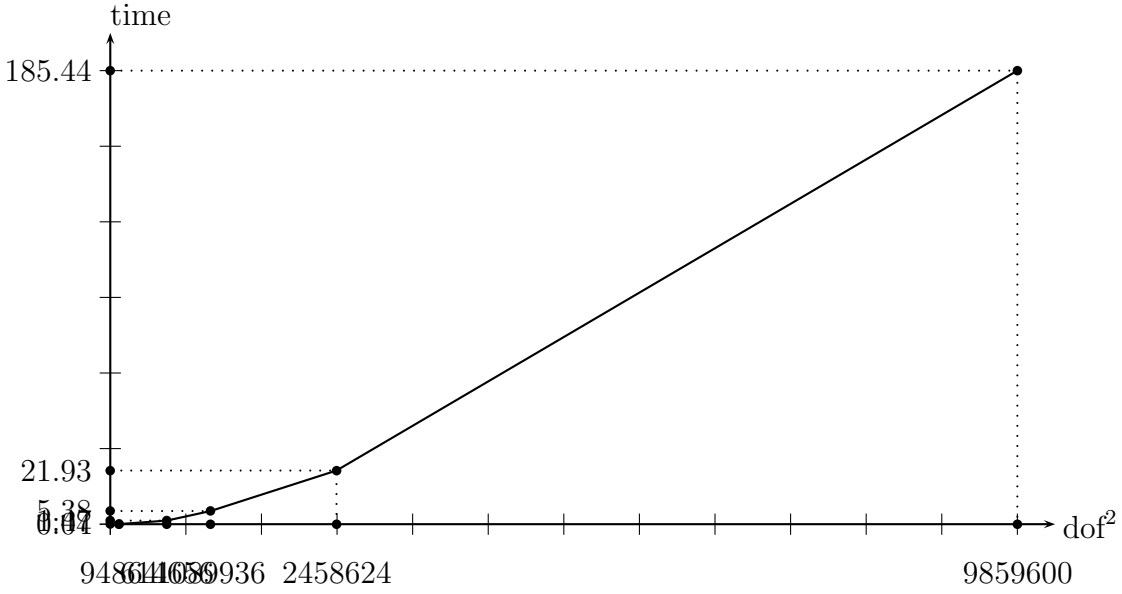

Figure 2.8: Relation between time needed to solve the system and dof.

Square problem

Here we have run the code written for smooth boundaries on a boundary mesh of a square of side $a = 5$ to which we prescribe $u = 0$ on the left side, $v = 1$ towards the outside

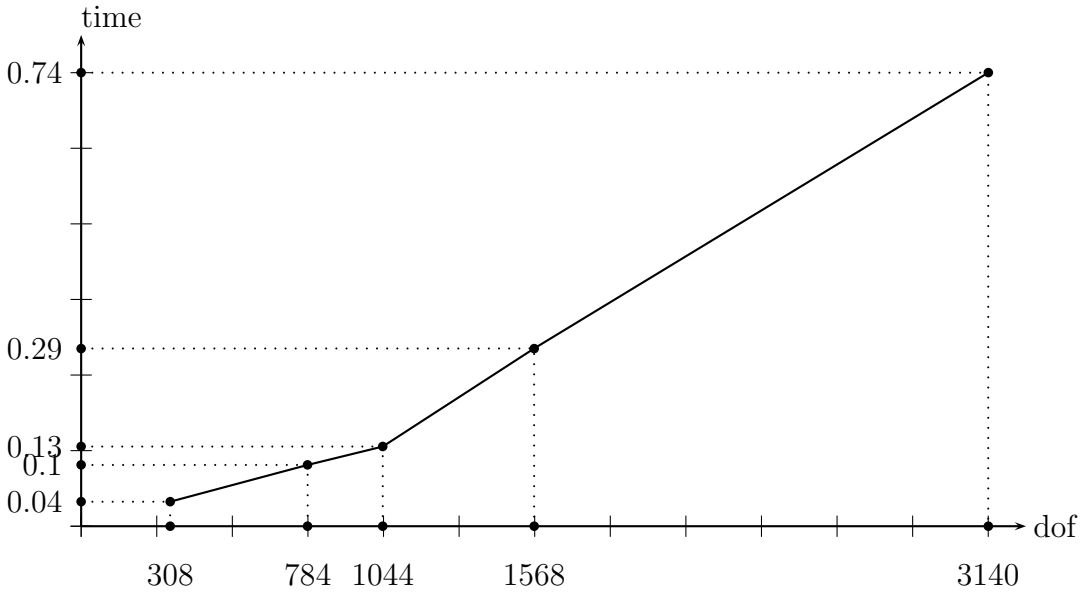

Figure 2.9: Relation between time needed to evaluate all points and dof.

normal vector of the right side, and $v = 0$ towards the outside normal vector of others sides. The analytical solution gives a field $u(x) = ax$ (see appendix D).

As can be seen in fig.(2.10), the error made on the points in the center of the domain is quite acceptable but the error becomes higher as we get closer to the corners. The flux is turning around the corners and the scale has been resized due to very high values : the highest values reach a norm of $4.83\ \ 10^3$ near the corners (high fluxes are saturated in fig.(2.10)).

The unaccuracy of those results is due to the fact that with constant elements, we cannot take into account the angles of the geometry as the nodes are located in the middle of the segments. Even if we had given a value to θ (see 2.1.3) and adapted the computation of G and H to an element bearing a geometrical singularity at the node, we would still need to give the same boundary condition at the right side and left side of the node. However, by refining the mesh around the corners, we slowly get closer to the analytical solution.

2.2.6 Conclusion on constant elements

To conclude, the BEM method using constant elements gives very good results for geometries with smooth boundaries (and requires much less time than FEM) but is unable to treat as well geometries with corners associated to different boundary conditions. As this drawback is due to the location of nodes at the middle of segments, we present in section

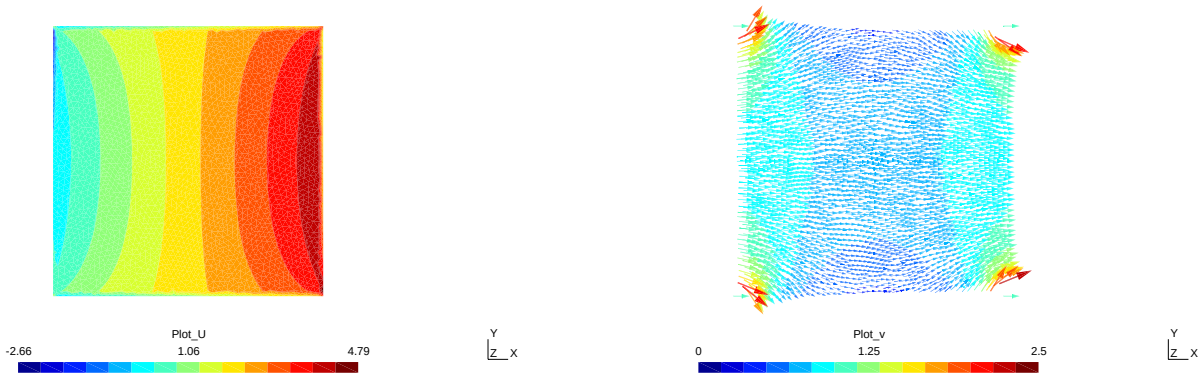

Figure 2.10: Field and flux on a simple square computed with constant elements

2.3 another discretization with nodes at the extremities of the elements.

Moreover, the precision on fluxes could be improved if the formulae given in section (2.2.3) were implemented instead of using finite differences.

2.3 Computation using linear elements

2.3.1 Discretization of the boundary

We approximate the boundary Γ with N segments Γ_j (where $j = 1, \ldots, N$) and locate the nodes at the extremities of those segments (see fig.(2.11)). Now the values u and v along a segment Γ_j are linearly interpolated from the values at its extremities using linear shape functions $\phi_1(s)$ and $\phi_2(s)$ (see fig.(2.12)) where s is the parameter used to describe an element (see 2.2.4).

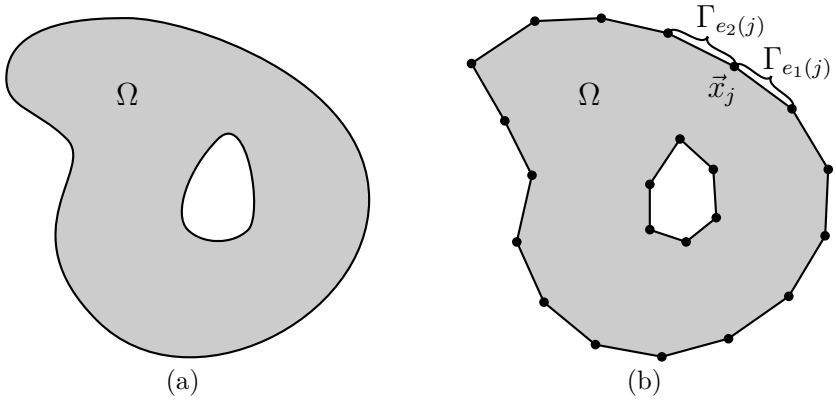

Figure 2.11: Discretization of a geometry (a) with linear elements (b).

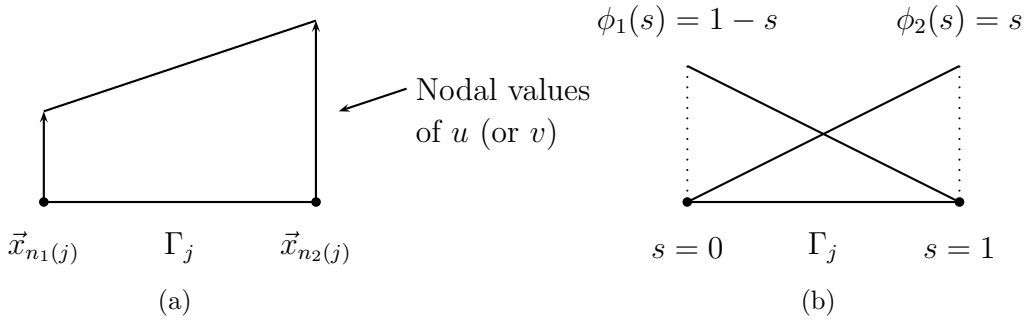

Figure 2.12: Interpolation with shape functions on a segment Γ_j.

For sake of clarity, we define the following mappings of indices:

$$\forall j \in [1, N], \quad \begin{array}{l} e_1(j) = \text{index of a segment connected to } \vec{x_j} \\ e_2(j) = \text{index of the other segment connected to } \vec{x_j} \\ n_1(j) = \text{index of a node at the end of } \Gamma_j \\ n_2(j) = \text{index of the other node at the end of } \Gamma_j \end{array}$$

As we work only with close geometries, the nodes are as numerous as the segments.

2.3.2 Types of boundary conditions

For a given j in $[1, N]$, three scalar values can be stored at a given node $\vec{x}_j$: the field at the node, noted u_j, and the two fluxes through the node respectively along the outward normal vectors to $\Gamma_{e_1(j)}$ and $\Gamma_{e_2(j)}$, noted v_1^j and v_2^j.

Let us list the different kinds of boundary conditions that can be given to a node $\vec{x}_j$:

	known value(s)	unknown(s)
a	v_1^j and v_2^j	u_j
b	v_1^j and u_j	v_2^j
c	u_j and v_2^j	v_1^j
d	u_j	v_1^j and v_2^j

We note $\{a\}$ the set of indices j such that node $\vec{x}_j$ has boundary conditions of type a (and similarly for $\{b\}$,$\{c\}$ and $\{d\}$).

In case d, there are two unknowns at one node so one extra equation is needed. This can be solved with techniques like discoutinuous elements (cf. Brebbia and Dominguez). In this thesis, we don't treat this case and run carefully the code on problems requiring only cases a, b and c. So in the following, $\sharp\{d\} = 0$.

2.3.3 Computation of the fields on the boundary

Equation (2.15) written for a node $\vec{x}_i$ becomes:

$$\begin{aligned}
(1 - \frac{\theta_i}{2\pi}\sigma_i)u_i &= \sum_{j=1}^{N} \Big(\int_{\Gamma_j} u^*(\vec{x}_i, \vec{x}) v(\vec{x}) d\Gamma(\vec{x}) \Big) - \sum_{j=1}^{N} \Big(\int_{\Gamma_j} v^*(\vec{x}_i, \vec{x}) u(\vec{x}) d\Gamma(\vec{x}) \Big) \\
&= \sum_{j=1}^{N} \Big(\int_{\Gamma_j} u^*(\vec{x}_i, \vec{x}) \Big[\phi_1(\vec{x}) v_{n_1(j)} + \phi_2(\vec{x}) v_{n_2(j)} \Big] d\Gamma(\vec{x}) \Big) \\
&\quad - \sum_{j=1}^{N} \Big(\int_{\Gamma_j} v^*(\vec{x}_i, \vec{x}) \Big[\phi_1(\vec{x}) u_{n_1(j)} + \phi_2(\vec{x}) u_{n_2(j)} \Big] d\Gamma(\vec{x}) \Big) \\
&= \sum_{j=1}^{N} \Big(\int_{\Gamma_{e_1(j)}} u^*(\vec{x}_i, \vec{x}) \phi_1(\vec{x}) d\Gamma(\vec{x}) \Big) v_j^1 + \sum_{j=1}^{N} \Big(\int_{\Gamma_{e_2(j)}} u^*(\vec{x}_i, \vec{x}) \phi_2(\vec{x}) d\Gamma(\vec{x}) \Big) v_j^2 \\
&\quad - \sum_{j=1}^{N} \Big(\int_{\Gamma_{e_1(j)}} v^*(\vec{x}_i, \vec{x}) \phi_1(\vec{x}) d\Gamma(\vec{x}) \Big) u_j - \sum_{j=1}^{N} \Big(\int_{\Gamma_{e_2(j)}} v^*(\vec{x}_i, \vec{x}) \phi_2(\vec{x}) d\Gamma(\vec{x}) \Big) u_j
\end{aligned}$$

We define:

$$G_{ij}^1 = \int_{\Gamma_{e_1(j)}} u^*(\vec{x}_i, \vec{x}) \phi_1(\vec{x}) d\Gamma(\vec{x}) \qquad G_{ij}^2 = \int_{\Gamma_{e_2(j)}} u^*(\vec{x}_i, \vec{x}) \phi_2(\vec{x}) d\Gamma(\vec{x}) \tag{2.28}$$

$$H_{ij}^1 = \int_{\Gamma_{e_1(j)}} v^*(\vec{x}_i, \vec{x})\phi_1(\vec{x})d\Gamma(\vec{x}) \qquad H_{ij}^2 = \int_{\Gamma_{e_2(j)}} v^*(\vec{x}_i, \vec{x})\phi_2(\vec{x})d\Gamma(\vec{x}) \tag{2.29}$$

Noting $H_{ij} = H_{ij}^1 + H_{ij}^2$, we get:

$$\begin{aligned}
(1 - \frac{\theta_i}{2\pi}\sigma_i)u_i &= \sum_{j=1}^{N} G_{ij}^1 v_j^1 + \sum_{j=1}^{N} G_{ij}^2 v_j^2 - \sum_{j=1}^{N} H_{ij}u_j \\
&= \sum_{j\in\{a\}} \Big(G_{ij}^1 \bar{v}_j^1 + G_{ij}^2 \bar{v}_j^2 - H_{ij}u_j \Big) \\
&\quad + \sum_{j\in\{b\}} \Big(G_{ij}^1 \bar{v}_j^1 + G_{ij}^2 v_j^2 - H_{ij}\bar{u}_j \Big) \\
&\quad + \sum_{j\in\{c\}} \Big(G_{ij}^1 v_j^1 + G_{ij}^2 \bar{v}_j^2 - H_{ij}\bar{u}_j \Big)
\end{aligned}$$

Then we can write the system:

$$\begin{pmatrix} H_{ik} & -G_{il}^2 & -G_{im}^1 \end{pmatrix} \begin{pmatrix} u_k \\ v_l^2 \\ v_m^1 \end{pmatrix} = \begin{pmatrix} G_{ik}^1 & -H_{il} & G_{im}^2 & G_{ik}^2 & G_{il}^1 & -H_{im} \end{pmatrix} \begin{pmatrix} \bar{v}_k^1 \\ \bar{u}_l \\ \bar{v}_m^2 \\ \bar{v}_k^2 \\ \bar{v}_l^1 \\ \bar{u}_m \end{pmatrix} \tag{2.30}$$

where k, l and m describe respectively $\{a\}$,$\{b\}$ and $\{c\}$. This is again a system of the form $\mathbf{Ax} = \mathbf{b}$. Once solved, we know the field and the flux everywhere on the boundary.

2.3.4 Computation of the fields anywhere inside the domain

Knowing the fields u and v anywhere on the boundary, we can compute the field u anywhere inside the domain thanks to eq.(2.10). The linear elements formulation of this equation is similar to eq.(2.28): $\forall \vec{y} \in \Omega\backslash\Gamma$,

$$\begin{aligned}
u(\vec{y}) &= \sum_{j=1}^{N} \Big(\int_{\Gamma_{e_1(j)}} u^*(\vec{y}, \vec{x})\phi_1(\vec{x})d\Gamma(\vec{x}) \Big) v_j^1 + \sum_{j=1}^{N} \Big(\int_{\Gamma_{e_2(j)}} u^*(\vec{y}, \vec{x})\phi_2(\vec{x})d\Gamma(\vec{x}) \Big) v_j^2 \\
&\quad - \sum_{j=1}^{N} \Big(\int_{\Gamma_{e_1(j)}} v^*(\vec{y}, \vec{x})\phi_1(\vec{x})d\Gamma(\vec{x}) \Big) u_j - \sum_{j=1}^{N} \Big(\int_{\Gamma_{e_2(j)}} v^*(\vec{y}, \vec{x})\phi_2(\vec{x})d\Gamma(\vec{x}) \Big) u_j
\end{aligned}$$

2.3.5 Computation of the fluxes anywhere

Knowing u and v anywhere on the boundary, we can compute the flux $\vec{v}$ anywhere inside the domain by discretizing eq.(2.11): $\forall \vec{y} \in \Omega$,

$$\begin{aligned}\vec{v}(\vec{y}) &= \sum_{j=1}^{N} \Big(\int_{\Gamma_{e_1(j)}} \vec{\nabla}_{\vec{y}}(u^*(\vec{x}_i,\vec{x}))\phi_1(\vec{x})d\Gamma(\vec{x}) \Big) v_j^1 + \sum_{j=1}^{N} \Big(\int_{\Gamma_{e_2(j)}} \vec{\nabla}_{\vec{y}}(u^*(\vec{x}_i,\vec{x}))\phi_2(\vec{x})d\Gamma(\vec{x}) \Big) v_j^2 \\ &\quad - \sum_{j=1}^{N} \Big(\int_{\Gamma_{e_1(j)}} \vec{\nabla}_{\vec{y}}(v^*(\vec{x}_i,\vec{x}))\phi_1(\vec{x})d\Gamma(\vec{x}) \Big) u_j - \sum_{j=1}^{N} \Big(\int_{\Gamma_{e_2(j)}} \vec{\nabla}_{\vec{y}}(v^*(\vec{x}_i,\vec{x}))\phi_2(\vec{x})d\Gamma(\vec{x}) \Big) u_j\end{aligned}$$

We define:

$$G_{ij}^{1v} = \int_{\Gamma_{e_1(j)}} \vec{\nabla}_{\vec{y}}(u^*(\vec{x}_i,\vec{x}))\phi_1(\vec{x})d\Gamma(\vec{x}) \qquad G_{ij}^{2v} = \int_{\Gamma_{e_2(j)}} \vec{\nabla}_{\vec{y}}(u^*(\vec{x}_i,\vec{x}))\phi_2(\vec{x})d\Gamma(\vec{x}) \quad (2.31)$$

$$H_{ij}^{1v} = \int_{\Gamma_{e_1(j)}} \vec{\nabla}_{\vec{y}}(v^*(\vec{x}_i,\vec{x}))\phi_1(\vec{x})d\Gamma(\vec{x}) \qquad H_{ij}^{2v} = \int_{\Gamma_{e_2(j)}} \vec{\nabla}_{\vec{y}}(v^*(\vec{x}_i,\vec{x}))\phi_2(\vec{x})d\Gamma(\vec{x}) \quad (2.32)$$

Due to a lack of time, the correct analytic formulae of G_{ij}^{1v}, G_{ij}^{2v}, H_{ij}^{1v} and H_{ij}^{2v} have not been written. So in the code, like for constant elements, the fluxes are computed using a finite difference. For dx and dy small enough, we compute:

$$\forall \vec{y} \in \Omega, \qquad v_x(\vec{y}) \approx \frac{u(\vec{y}+dx\vec{e}_x) - u(\vec{y})}{dx} \qquad \text{and} \qquad v_y(\vec{y}) \approx \frac{u(\vec{y}+dy\vec{e}_y) - u(\vec{y})}{dy} \quad (2.33)$$

Again, a special care is taken to choose the size and the sign of dx and dy in order that $\vec{y}+dx\vec{e}_x$ and $\vec{y}+dy\vec{e}_y$ stay inside the domain.

2.3.6 Test cases

In order to justify the use of linear elements instead of constant elements, we first work on the case of the square leading to unaccurate results with constant elements. Then we add a centered hole (various shape) to this problem. Finally, the formulation is tested on a more complex problem (for which the analytic solution is not known) in order to check that the accuracy of the computation is not due to the simplicity of the test cases.

Square problem

As the analytical solution is linear, the linear elements are theoritically able to describe the exact solution. We run exactly the same test as done previously with constant elements described in (2.2.5). Numerically, we get a precision of 10^{-12} (the machine precision) using a boundary mesh of only 4 nodes (the corners of the square) as can be seen in fig.(2.13).

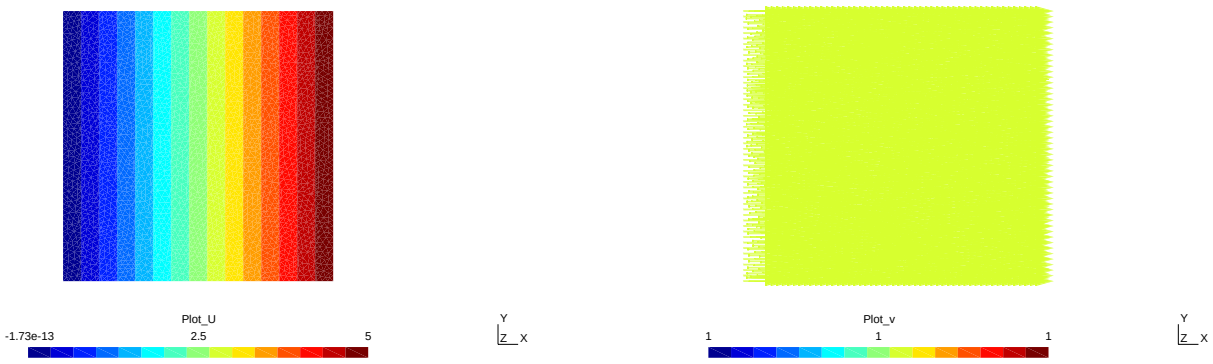

Figure 2.13: Solution on a simple square with linear elements

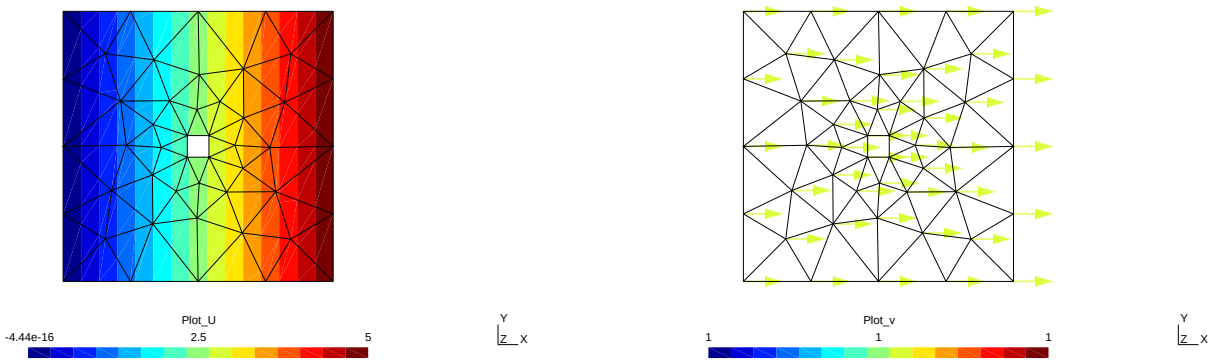

Figure 2.14: Square with a square hole

Square problem with a hole

Now we add a square hole in the center of the domain. As we impose the same boundary conditions on the small square as on the external square, the hole should not disturb the solution. It is a way to check that the formulation is able to treat an internal boundary correctly. Again, we obtain the analytic solution to the machine precision as can be seen in fig.(2.14).

Then we do the same test with an octogonal hole in order to check that the angle is taken into account at corners correctly. The boundary conditions are also such that the inclusion should not disturb the solution. Again, we obtain the analytic solution to the machine precision as can be seen in fig.(2.15).

Then we do the same test on a rectangle with a circular hole. To get a nice repre-

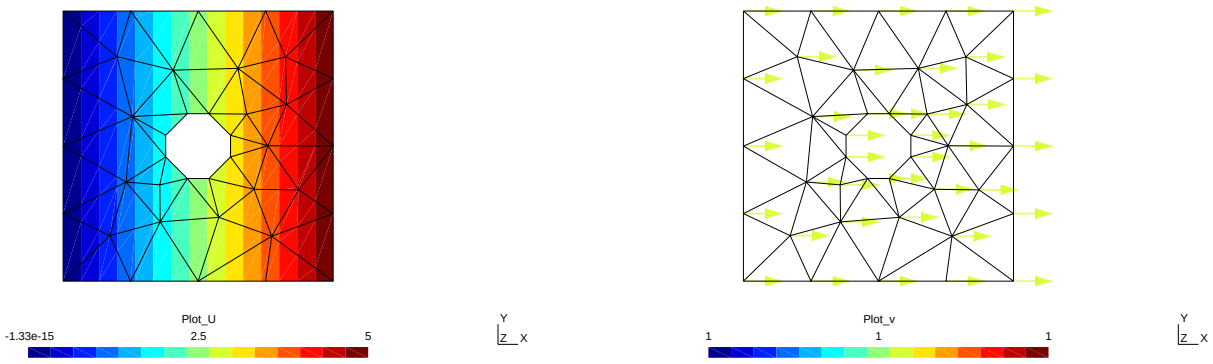

Figure 2.15: Square with an octogonal hole

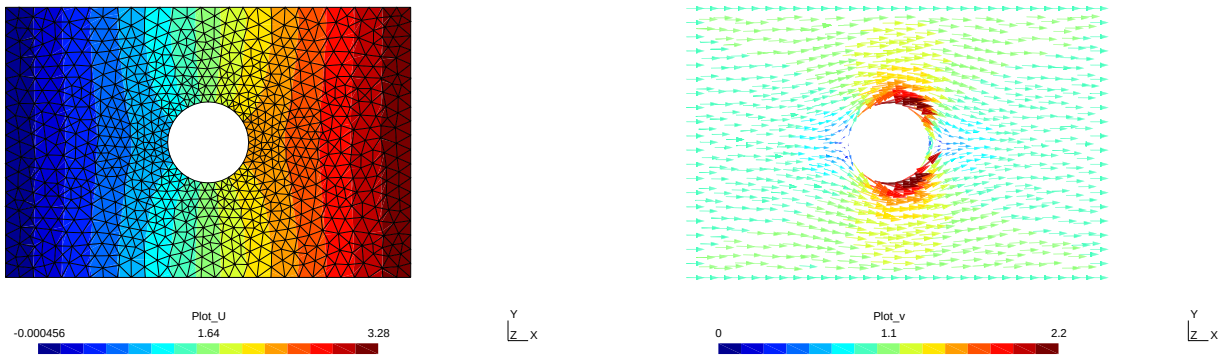

Figure 2.16: Rectangle with a circular hole

sentation of the curvature of the circle and avoid boundary conditions of type (d) (see 2.3.2), we impose the normal flux to be zero on the boundary of the hole. This time, the inclusion should disturb the field such that the solution is not linear anymore (the analytic solution is not known).

In this example, due to the choice of boundary conditions, we can refine the mesh of the boundary of the hole whereas the previous test cases run with 4, 8 and 12 nodes respectively on the boundary (located at corners). The computational time has been evaluated on three different refinements:

number of dof on the boundary	number of dof in the domain	time			
		fill matrices	solve the system	evaluate inside	total
40	951	0.01s	<0.01s	0.51s	0.52s
380	951	0.82s	0.12s	5.11s	6.05s
1888	951	28.28s	42.45s	28.31s	99.04s

For a comparable number of nodes on the boundary, the BEM formulation using linear elements requires more time than the one using constant elements (see section (2.2.5)), but it stays satisfactory.

Complex problem

Finally, we work on a more complex case with several inclusions. The analytic solution is not known for this kind of geometry. Here again, we impose the normal flux to be zero on all internal boundaries to avoid boundary conditions of type (d) (see section 2.3.2).

The localization of the flux on the two nodes on the right (see fig.(2.3.2)) can be explained by the boundary conditions. Indeed, we imposed the normal flux to be zero on the upper and lower boundaries whereas it is imposed to be 1 on the arc of circle on the right. As the geometry is smooth[2] at the junction of the different conditions, we introduced a discontinuity on the flux in the $\vec{e_y}$ direction.

2.3.7 Conclusion on linear elements

To conclude, the BEM method using linear elements is as satisfactory as constant elements in terms of time performance and is able to treat well geometries with corners.

However, the computation of the fluxes should be even more precise if the formulae given in section (2.2.3) were implemented instead of using finite differences[3].

A big weakness of the code is the fact that boundary conditions of type (d) are not treated. Consequently, the user should take care to never impose Dirichlet boundary conditions on two joined segments. This reduces drastically the cases which can be treated. When coupling with the crack propagation code, as the boundary of the crack front is a free curve (surface in 3D), we will impose a Newman boundary condition ($v = 0$) all over the inner boundary so the linear elements will be used safely.

[2]Once discretized, the geometry is not exactly smooth, but the finer is the mesh, the closer are the outside unit normal vectors of the segments connected to the nodes of interest.

[3]The analytical evaluation of the integrals required for this computation is possible, but have not been achieved correctly during this master thesis (see section (2.3.5))

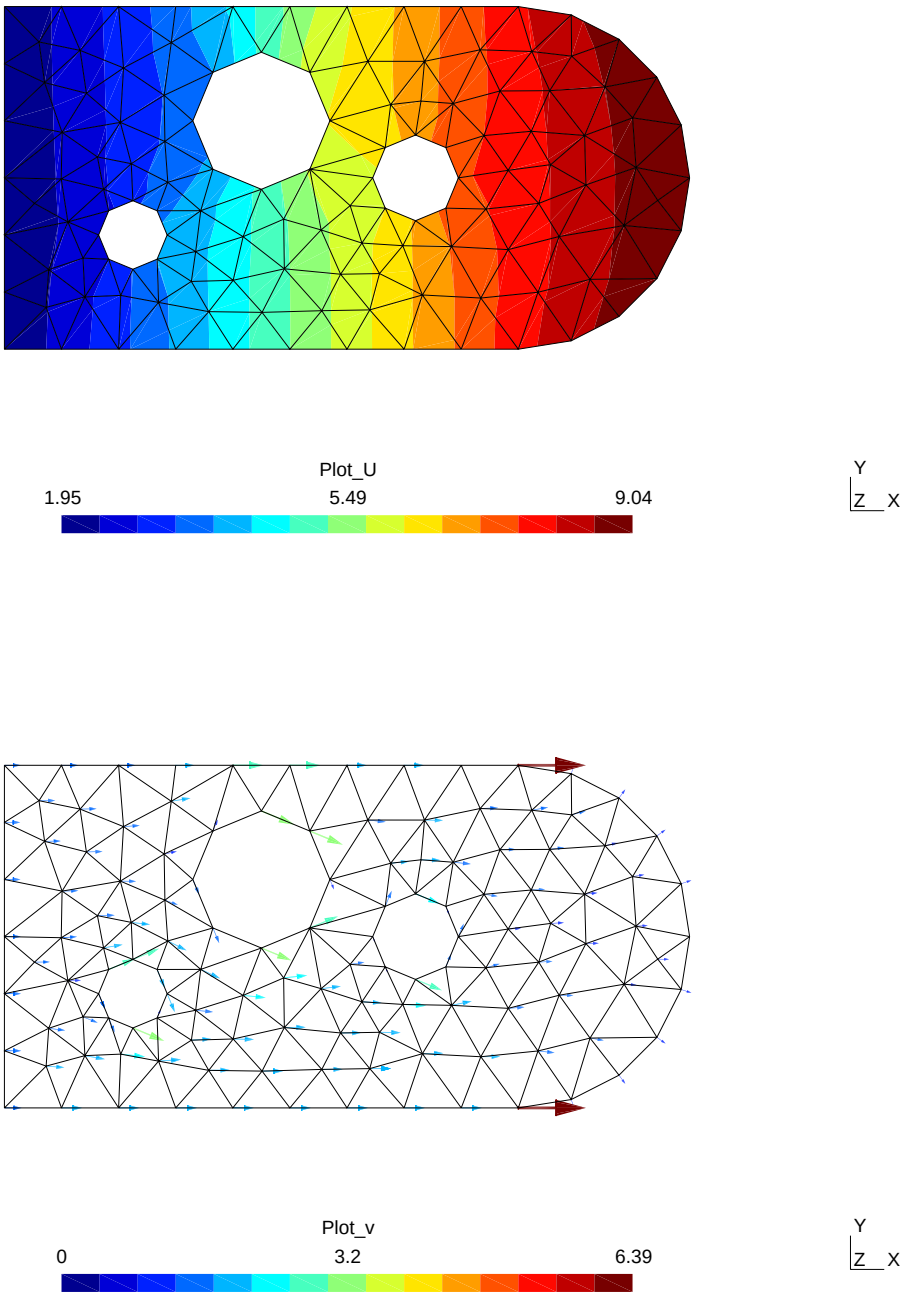

Figure 2.17: Complex geometry problem

Chapter 3

Crack propagation

3.1 Brittle damage

The damage is called brittle because a virgin zone (in which the damage is $d = 0$) is separated by a front from a totally damaged zone in which $d = 1$. The boundary of the damaged zone is a curve (or a surface in three-dimensionnal problems) with a discontinuity of stress. It is also a free curve for the virgin zone because the normal stress is zero there[1].

An alternative representation is for instance a continuous description of the damage using a multiphase level set [21].

3.2 Propagation criteria

The model of propagation used here is a Griffith type criteria. The front is growing provided the energy released is equal to a critical energy plus a term involving the front curvature as explained by N.Moës in [14]. The presence of the curvature is essential for the model to avoid spurious localization.

The model considered is the one introduced by Q.S.Nguyen in [16]. We consider an elastic domain Ω submitted to imposed loads $\vec{T}(\vec{x}, \lambda)$ and displacements $\vec{u}(\vec{x}, \lambda)$ on the part of the boundary Γ_T and Γ_U, respectively. The parameter λ is the loading parameter (carrying information about the history of loading) and we assume that the imposed loads and displacements depend linearly on λ, i.e. $\vec{T}(\vec{x}, \lambda) = \lambda \vec{t}^0(\vec{x})$ and $\vec{U}(\vec{x}, \lambda) = \lambda \vec{u}^0(\vec{x})$.

The space of admissible displacement field is denoted as U and the space of admissible displacement field to zero is denoted as U_0.

The complementary part of the boundary delimiting the completely damaged and

[1] This allows us to impose the normal "flux" to be zero on the crack propagation front. This way, we ensure to avoid the type d of boundary conditions and we can use the linear elements safely.

virgin material is denoted Γ. The potential energy in the system is given by:

$$E(\Gamma, \vec{u}, \lambda) = \int_\Omega e d\Omega - \int_{S_T} \lambda \vec{t}^0 \cdot \vec{u} dS \tag{3.1}$$

$$\text{with } e = \frac{1}{2}\boldsymbol{\epsilon}(\vec{u}) : \boldsymbol{E} : \boldsymbol{\epsilon}(\vec{u}) \text{ and } \vec{u} = \lambda \vec{u}^0 \text{ on } S_u \tag{3.2}$$

where $\boldsymbol{E}$ is Hooke's tensor. The displacement field $\vec{u} \in U$ is obtained through the stationarity of the functional:

$$\int_\Omega \boldsymbol{\epsilon}(\vec{u}) : \boldsymbol{E} : \boldsymbol{\epsilon}(\vec{u}^*) d\Omega = \int_{S_T} \lambda \vec{t}^0 \cdot \vec{u} dS \qquad \forall \vec{u}^* \in U_0 \tag{3.3}$$

Its solution depends on the current degradation front location and load factor:

$$\vec{u} = \vec{u}(\Gamma, \lambda) \tag{3.4}$$

The free energy of the system at equilibrium is denoted W:

$$W(\Gamma, \lambda) = E(\Gamma, \vec{u}(\Gamma, \lambda), \lambda) \tag{3.5}$$

Assuming a normal velocity q_n modifying the location of the front, the free energy will be altered. Assuming the front is regular, the directional derivative of the free energy with respect to the velocity q_n is written:

$$DW[q_n] = -\int_\Gamma e q_n dS \tag{3.6}$$

The dual quantity to q_n on the front is the energy release rate e. The brittle propagation law is given by:

- If $e < Y_C + \frac{\gamma_c}{\rho}$, the propagation is impossible
- If $e = Y_C + \frac{\gamma_c}{\rho}$, the propagation is possible

The degradation front will move forward if the elastic energy on the front is superior to a critical energy Y_C plus a critical surface energy times the front curvature.

3.3 Evaluation of the elastic energy on the front

Until now, an Xfem code was used to compute the elastic energy on the front. This level set approach is also used by [19] with an iterative Fourier spectral method.

For the mode III problem studied here, the elastic energy is computed as:

$$E(\vec{x}) = \frac{1}{2}\mu \vec{v}(\vec{x}) \cdot \vec{v}(\vec{x}) \tag{3.7}$$

where $\vec{v}(\vec{x})$ is the flux computed by the BEM formulation at point $\vec{x}$ and μ is a parameter set to one in the following.

3.4 Construction of the boundary mesh

The boundary mesh sent to the BEM formulation is constructed with the nodes at the intersection of the domain mesh and the level set. It is updated at each iteration. Once out of ten iterations, the domain mesh is updated: the areas of interest are refined and some becomes coarser. The refinement of the mesh is limited by a parameter p such that a cell cannot be refine more than p times.

3.5 Test cases

We have been confronted to some round-off problems, which are still not solved. To circumvent them, we have multiplied the dimension of the problem by a factor 1000.

We have run the test of a square plane of side 1000 with one or several circular hole(s). p is set to 7 for the run of all test cases, meaning that the smallest cell of the domain mesh has a side of $1000/2^7 = 7,8125$.

As illustrated by fig.(3.1), the boundary conditions applied are:

- on the right side: $u = 0$
- on the left side: $u = 100$
- on the upper and lower sides and inner boundaries: $v = 0$ towards the outside of the domain

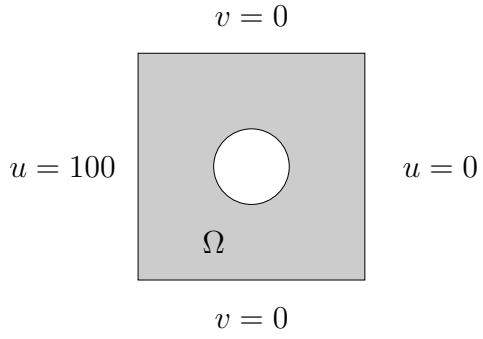

Figure 3.1: Boundary conditions of the test case

3.5.1 One circular hole

In fig.(3.2), you can see the field of displacement computed by the FEM formulation at the beginning of the run and then every ten iterations. You can see on the two last pictures the beginning of a spurious localization, proof that this phenomenon is not prevented

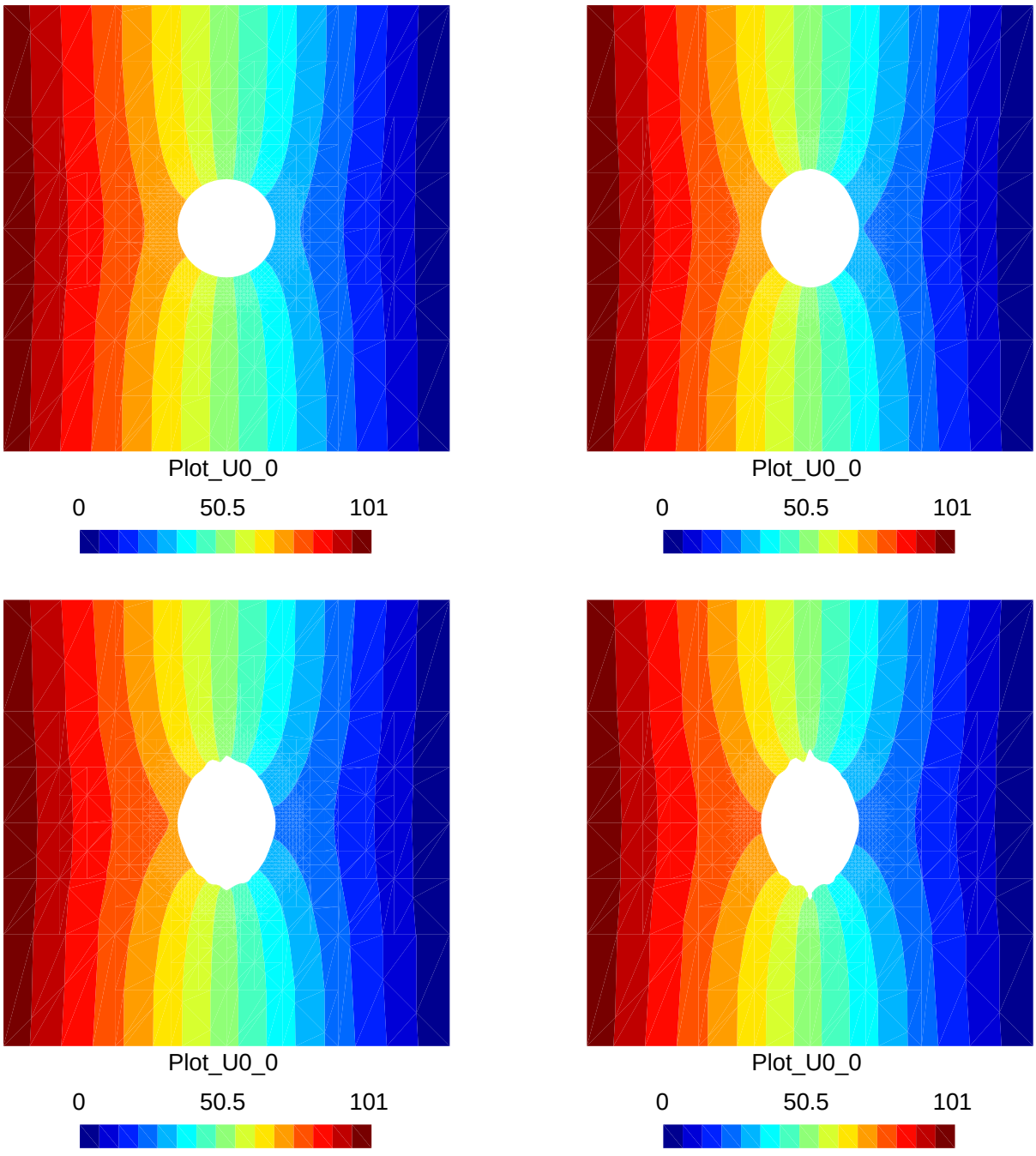

Figure 3.2: Evolution of the displacement and propagation of the front.

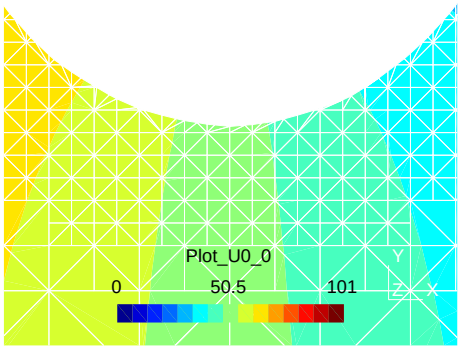

Figure 3.3: Detail of the front before localization.

by the use of a BEM. Let us note that we study a highly unstable case. According to E.Taroco [20], the crack advance stability is influenced by the first- and higher- order potential energy release rates.

Let us remark that the loss of symmetry happens before the localization. Indeed, you can see on the second picture of fig.(3.2) that the isolines of displacements behave differently on the left or right side. At this step, there is no localization though, as illustrated in fig.(3.3).

If we let the computation goes on, we can get the extreme configuration of fig.(3.4) (obtained after 669 iterations). B.Fedelich and A.Ehrlacher have written necessary condition for stability in [8] and [9]. We could use their work to know if a path is acceptable crack propagation.

You can also remark that the crack has a caracteristic width when it propagates. This width could be related to the size of the smallest element of the mesh. This shows that this computation is not absolutly independant of the mesh.

In fig.(3.5), the localization has been observed closely on two consecutive iterations. On the first picture, the tip of the crack is very close to a node of the mesh and the intersection of the level set and the mesh produces very small segments near the tip. After another iteration, the propagation front has moved a lot whereas the gradient of displacement did not seem to justify such a move. We can interpret this behaviour by the fact that the flux is computed by finite differences. In particular, the flux at a point of the boundary is computed as the difference of the fields at the two nodes of the segment to which the point belongs, divided by the length of the segment. Consequently, the smaller is the length of the segment, the less precise is the computation of the flux. This could explain also why the directions of the mesh are priviledged directions for the propagation of the crack (see fig.(3.4)).

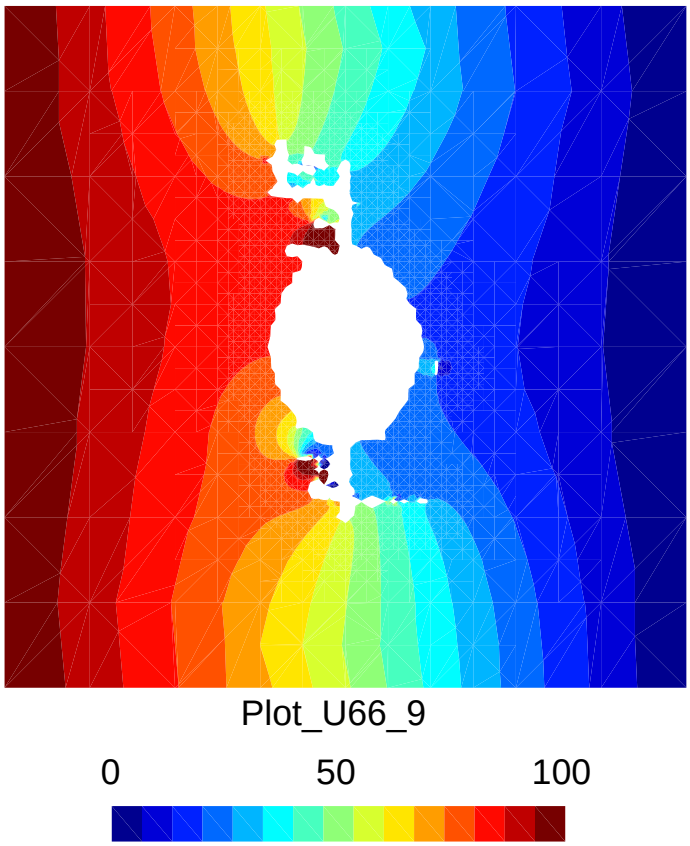

Figure 3.4: Last iteration computed before stoping the run.

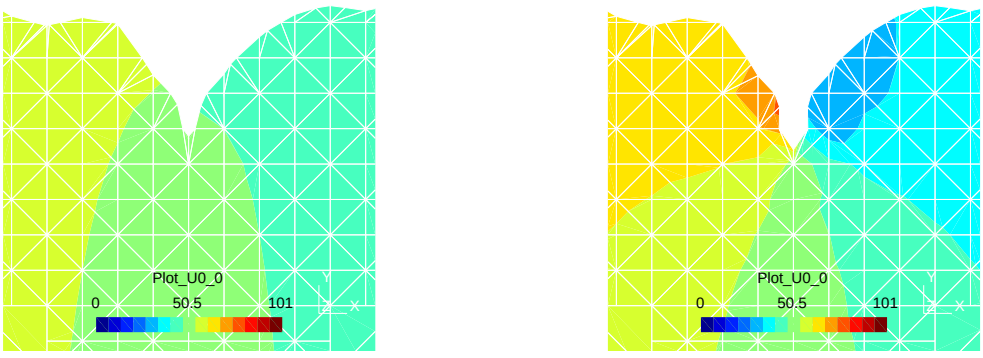

Figure 3.5: Localized propagation of the front.

3.5.2 Two circular holes

Now we study the same square but with two holes near the center such that the two propagation fronts can merge. In fig.(3.6), you can see the field of displacement computed by the FEM formulation at the beginning of the run and then every four iterations. The propagation front stays very smooth and the merging of the two fronts works.

Once the two holes have merged, the propagation of the fronts goes on in the y direction, then the symmetry is lost (one front is more advanced than the other) and localization happens as can be seen in fig.(3.7) (obtained after 43 iterations). Here again, you can remark that the top localized crack propagates in a direction of the mesh (y), with a width comparable to the size of the smallest segment of the domain mesh.

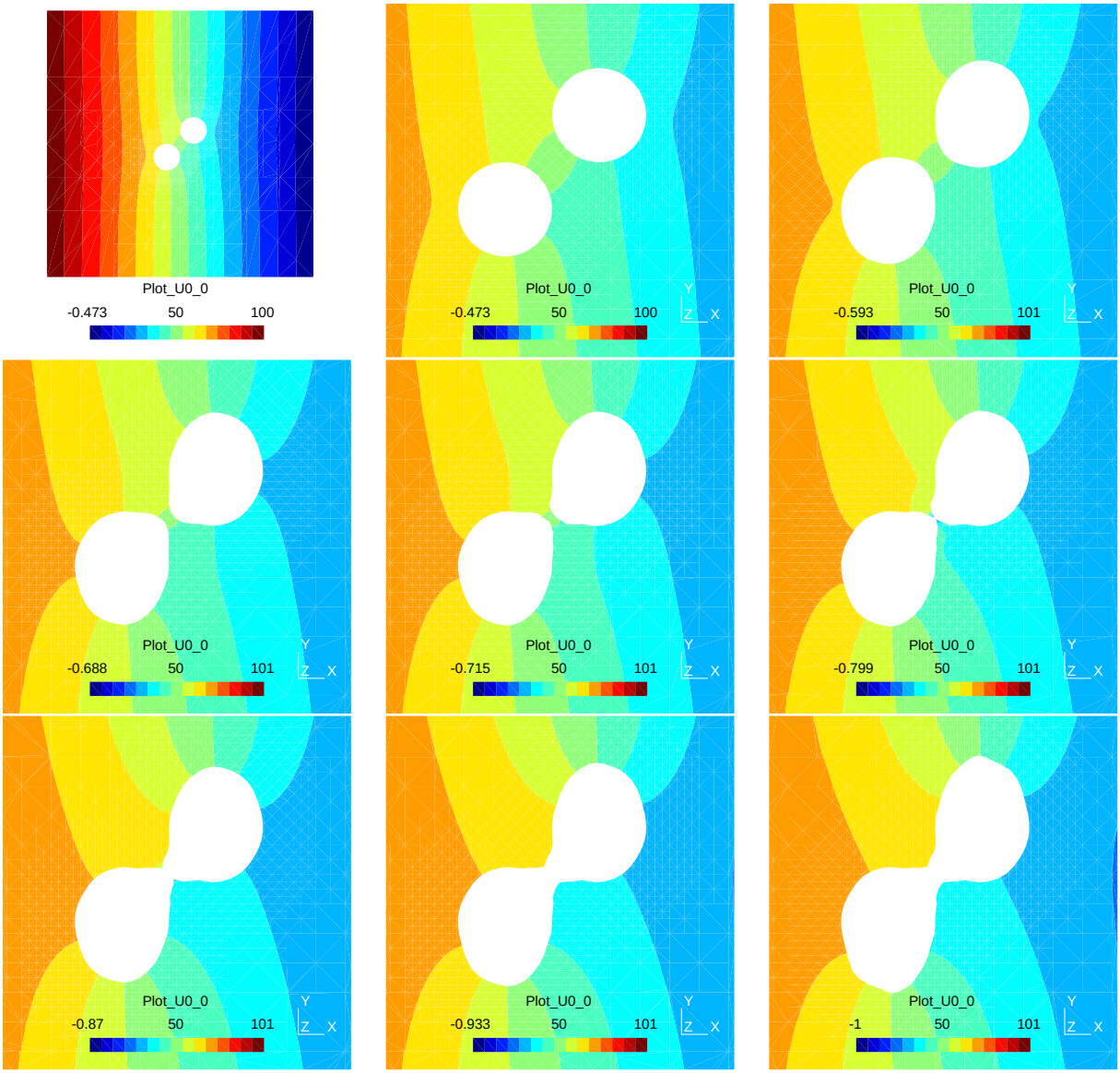

Figure 3.6: Evolution of the displacement and propagation of the front.

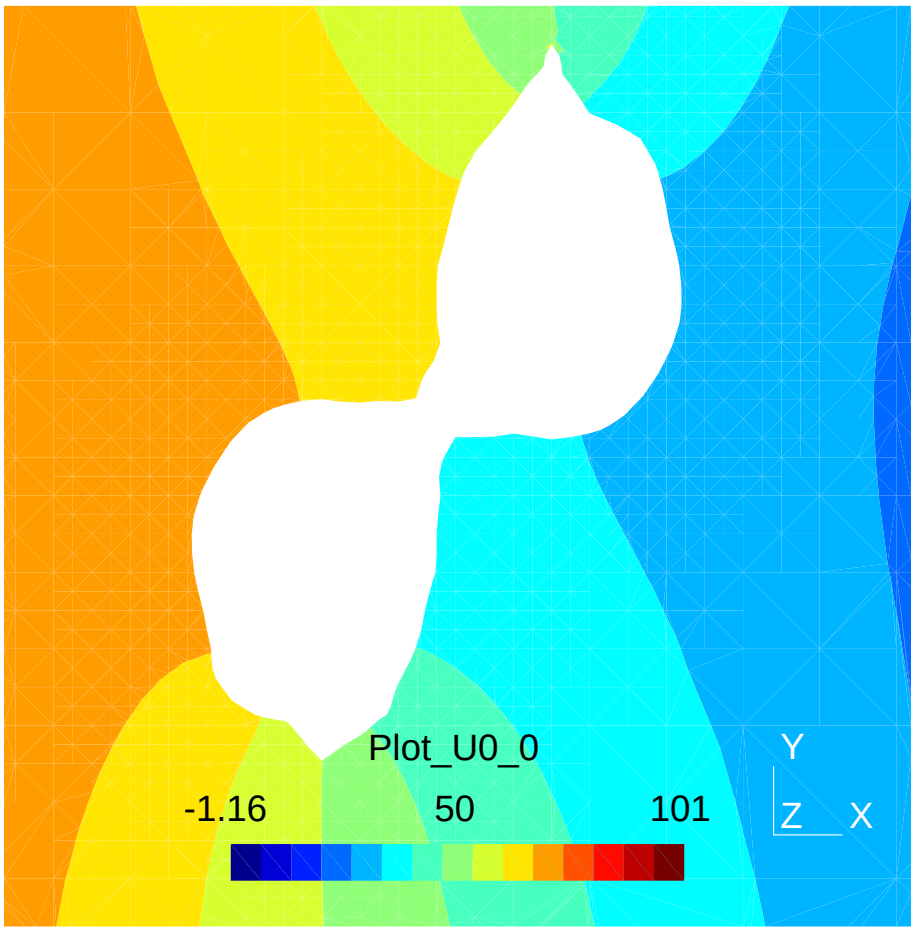

Figure 3.7: Last iteration computed before stoping the run.

Conclusion and prospects

To conclude this master thesis, I have implemented a BE formulation which is able to compute the elastic energy on the boundary for a mode III problem in 2D. Then this formulation has been coupled to a propagation code which uses this energy to evaluate a propagation criteria. We have observed by running test cases that the BEM formulation is able to compute the propagation of the front without localization for a few iterations. This was not achieved by the FEM. It can also merge successfully two propagation fronts. We can assume that those results would be still improved if the BEM formulation computed the flux (which is required to evaluate the elastic energy) more precisely by using an integral formulation instead of a finite difference.

I would like to notice that the BEM yields to matrices which are more difficult to interpret than the FEM ones and the debugging part of my work took a lot of time. To finish in the imparted time, I had to choose to skip interesting developments but I am satisfied to have run the BE code coupled with the crack propagation and note that the BEM brings new results.

To continue the started work, it would be useful to change the implementation of the BEM such that the Dirichlet boundary conditions are imposed on nodes instead of elements, to allow boundary conditions of type (d) with linear elements (using discontinuous elements like C.A.Brebbia [3] for instance), to code the computation of fluxes using the integral formulation instead of a finite difference, to clean the code to avoid round-off problems, to optimize the implementation in order to save more time, and to identify if the localization is intrinsically related to the method.

Appendix A

Matrices computed for constant elements

The integrated functions in G_{ij} and H_{ij} are always bounded, excepted when $\vec{p}_i$ belongs to Γ_j, which happens if and only if[1] $i = j$. In the following, we will treat the general case first, then the diagonal terms.

A.1 Preliminar statements

The litteral expression of G and H depends on the sign of the determinant $D = \beta^2 - 4\alpha\gamma$ of the second order polynom $r_{ij}^2(s)$.

$$\begin{aligned}
D_{ij} &= \beta_{ij}^2 - 4\alpha_{ij}\gamma_{ij} \\
&= 4\Big((x_1^j - \frac{x_1^i + x_2^i}{2})(x_2^j - x_1^j) + (y_1^j - \frac{y_1^i + y_2^i}{2})(y_2^j - y_1^j)\Big)^2 \\
&\quad -4\Big(\Big(x_1^j - \frac{x_1^i + x_2^i}{2}\Big)^2 + \Big(y_1^j - \frac{y_1^i + y_2^i}{2}\Big)^2\Big)\Big((x_2^j - x_1^j)^2 + (y_2^j - y_1^j)^2\Big) \\
&= 4\Big[2(x_1^j - \frac{x_1^i + x_2^i}{2})(x_2^j - x_1^j)(y_1^j - \frac{y_1^i + y_2^i}{2})(y_2^j - y_1^j) \\
&\quad -\Big(x_1^j - \frac{x_1^i + x_2^i}{2}\Big)^2(y_2^j - y_1^j)^2 - \Big(y_1^j - \frac{y_1^i + y_2^i}{2}\Big)^2(x_2^j - x_1^j)^2\Big] \\
&= -4\Big[\Big(x_1^j - \frac{x_1^i + x_2^i}{2}\Big)(y_2^j - y_1^j) - \Big(y_1^j - \frac{y_1^i + y_2^i}{2}\Big)(x_2^j - x_1^j)\Big]^2
\end{aligned}$$

$$\text{Noting} \qquad \vec{n}(\vec{p_1}^j, \vec{p_2}^j) = \begin{pmatrix} y_2^j - y_1^j \\ x_1^j - x_2^j \end{pmatrix} \qquad \text{we have} \qquad D = -4\Big(\vec{n}(\vec{p_1}^j, \vec{p_2}^j) \cdot \overrightarrow{p^i p_1^j}\Big)^2 \quad \text{(A.1)}$$

[1] We assume that the mesh doesn't cross itself.

$\vec{n}(\vec{p_1}^j, \vec{p_2}^j)$ is a normal vector to $\overrightarrow{p_1^j p_2^j}$. So D is negative and reachs zero if and only if $\vec{p_1}^j, \vec{p_2}^j$ and $\vec{p}^{\,i}$ are colinear. This happens in particular when $i = j$:

$$\begin{aligned}
\alpha_{ii} &= \Big(\frac{x_1^i - x_2^i}{2}\Big)^2 + \Big(\frac{y_1^i - y_2^i}{2}\Big)^2 = \frac{\gamma_{ii}}{4} \\
\beta_{ii} &= 2\Big((\frac{x_1^i - x_2^i}{2})(x_2^i - x_1^i) + (\frac{y_1^i - y_2^i}{2})(y_2^i - y_1^i)\Big) \\
&= -\Big((x_1^i - x_2^i)^2 + (y_1^i - y_2^i)^2\Big) \\
&= -\gamma_{ii} \\
D_{ii} &= \beta_{ii}^2 - 4\alpha_{ii}\gamma_{ii} = (-\gamma_{ii})^2 - 4\frac{\gamma_{ii}}{4}\gamma_{ii} \equiv 0
\end{aligned}$$

As $\vec{n}(\vec{p_1}^j, \vec{p_2}^j)$ is easy to compute, we use it to express $\vec{n}_j$, the unit normal vector to Γ_j pointing outward[2]. We define the function s such that $s(\vec{p_1}^j, \vec{p_2}^j)$ describes if $\vec{n}(\vec{p_1}^j, \vec{p_2}^j)$ is pointing inward or outward the boundary to which Γ_j belongs (see fig.(A.1)):

$$s(\vec{p_1}^j, \vec{p_2}^j) = \begin{cases} +1 & \text{if } \vec{p_1}^j \text{ and } \vec{p_2}^j \text{are numbered clockwise} \\ -1 & \text{if } \vec{p_1}^j \text{ and } \vec{p_2}^j \text{are numbered anticlockwise} \end{cases} \tag{A.2}$$

Noting $s_j = s(\vec{p_1}^j, \vec{p_2}^j)$ and $\vec{n}_j = \vec{n}(\vec{p_1}^j, \vec{p_2}^j)$, we have:

$$\vec{n}^e = \frac{\sigma_j s_j}{\|\overrightarrow{p_1^j p_2^j}\|}\vec{n}(\vec{p_1}^j, \vec{p_2}^j) = \frac{\sigma_j s_j}{\sqrt{\gamma}}\vec{n}(\vec{p_1}^j, \vec{p_2}^j) \tag{A.3}$$

A.2 Computation of G_{ij}

$$G_{ij} = \int_0^1 -\frac{ln(\alpha + \beta s + \gamma s^2)}{4\pi}\sqrt{\gamma}ds$$

Integration by part:

$$\begin{aligned}
&f' = 1 && f = s \\
&g = ln(\alpha + \beta s + \gamma s^2) && g' = \tfrac{\beta + 2\gamma s}{\alpha + \beta s + \gamma s^2}
\end{aligned}$$

$$G_{ij} = -\frac{\sqrt{\gamma}}{4\pi}\Big(\Big[sln(|\alpha + \beta s + \gamma s^2|)\Big]_0^1 - \int_0^1 \frac{\beta s + 2\gamma s^2}{\alpha + \beta s + \gamma s^2}ds\Big)$$

[2]The orientation of the unit outside normal vector is complex because we work only with a mesh of a boundary. Once the BEM formulation is coupled with the propagation code, the orientation of those vectors are easily computed thanks to the level set.

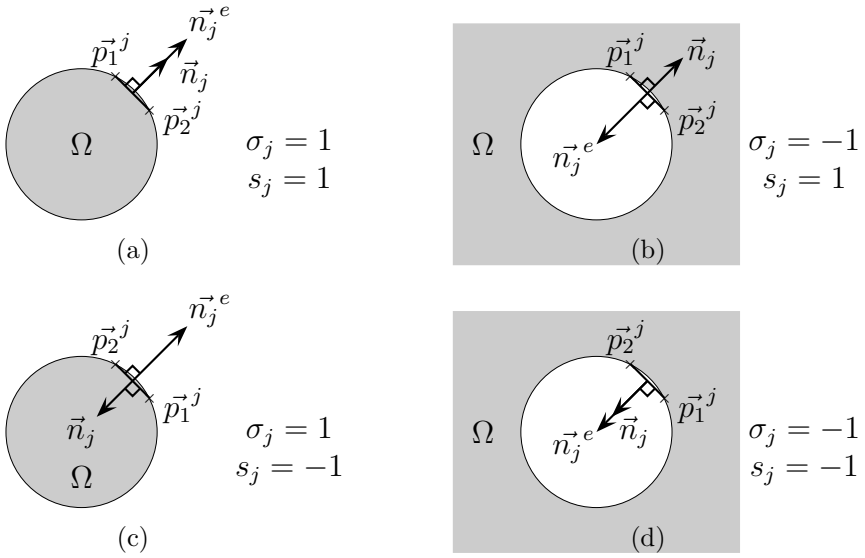

Figure A.1: $\vec{n}_j$ and $\vec{n_j}^e$ for different values of s_j and σ_j.

Decomposition of the rationnal function:

$$\begin{aligned}
\frac{\beta s + 2\gamma s^2}{\alpha + \beta s + \gamma s^2} &= 2 - \frac{\beta s + 2\alpha}{\alpha + \beta s + \gamma s^2} \\
&= 2 - \Big(\frac{\beta}{2\gamma}\Big)\frac{\beta + 2\gamma s}{\alpha + \beta s + \gamma s^2} - \Big(2\alpha - \frac{\beta^2}{2\gamma}\Big)\frac{1}{\alpha + \beta s + \gamma s^2} \\
&= 2 - \Big(\frac{\beta}{2\gamma}\Big)\frac{\beta + 2\gamma s}{\alpha + \beta s + \gamma s^2} - \Big(\frac{-D}{2\gamma}\Big)\frac{1}{\alpha + \beta s + \gamma s^2} \qquad \text{(A.4)}
\end{aligned}$$

We define:

$$I_0 = \int_0^1 \frac{1}{\alpha + \beta s + \gamma s^2} ds \qquad \text{and} \qquad I_1 = \int_0^1 \frac{\beta + 2\gamma s}{\alpha + \beta s + \gamma s^2} ds$$

$$G_{ij} = -\frac{\sqrt{\gamma}}{4\pi}\Big(\Big[sln(|\alpha + \beta s + \gamma s^2|) - 2s\Big]_0^1 + \frac{\beta}{2\gamma} I_1 + \frac{-D}{2\gamma} I_0\Big)$$

After computation of integrals I_0 and I_1 (detailled in section (C)), we get:

$$\begin{aligned}
\text{if } D<0 \qquad G_{ij} &= -\frac{\sqrt{\gamma}}{4\pi}\Big[\Big(s+\frac{\beta}{2\gamma}\Big)ln(|\alpha+\beta s+\gamma s^2|)-2s+\frac{\sqrt{-D}}{\gamma}arctan\Big(\frac{\beta+2\gamma s}{\sqrt{-D}}\Big)\Big]_0^1 \\
&= -\frac{\sqrt{\gamma}}{4\pi}\Big[\Big(1+\frac{\beta}{2\gamma}\Big)ln(|\alpha+\beta+\gamma|)-\frac{\beta}{2\gamma}ln(\alpha)-2 \\
&\quad +\frac{\sqrt{-D}}{\gamma}\Big(arctan\Big(\frac{\beta+2\gamma}{\sqrt{-D}}\Big)-arctan\Big(\frac{\beta}{\sqrt{-D}}\Big)\Big)\Big] \\
\text{if } D=0 \qquad G_{ij} &= -\frac{\sqrt{\gamma}}{4\pi}\Big[ln(|\alpha+\beta+\gamma|)-2+\frac{\beta}{\gamma}ln\Big(\Big|\frac{2\gamma}{\beta}+1\Big|\Big)\Big]
\end{aligned}$$

For diagonal terms, we deal with the case $D=0$, and as $\beta=-\gamma$ in particular, we have:

$$G_{ij}=-\frac{\sqrt{\gamma}}{4\pi}\Big(ln(\alpha)-2\Big)=\frac{\sqrt{\gamma}}{2\pi}\Big(ln(\frac{1}{\sqrt{\alpha}})+1\Big)=\frac{\sqrt{\gamma}}{2\pi}\Big(ln(\frac{2}{\sqrt{\gamma}})+1\Big)$$

A.3 Computation of H_{ij}

$$H_{ij} = \int_0^1 -\frac{\sqrt{\gamma}}{2\pi r(s)}\vec{e_r}(s).\vec{n}_j^e ds$$

$$\begin{aligned}
\vec{e_r}(s).\vec{n}_j^e &= \frac{(\vec{p}^i-\vec{p}^j(s))}{r(s)}.\vec{n}_j \\
&= \frac{1}{r(s)}\Big(\Big(x_i-(x_1^j+s(x_2^j-x_1^j))\Big)n_j^x+\Big(y_i-(y_1^j+s(y_2^j-y_1^j))\Big)n_j^y\Big) \\
&= \frac{1}{r(s)}\Big((x_i-x_1^j)n_j^x+(y_i-y_1^j)n_j^y-s((x_2^j-x_1^j)n_j^x+(y_2^j-y_1^j)n_j^y)\Big)
\end{aligned}$$

As $\vec{n}_j$ is normal to $\vec{p}_2-\vec{p}_1$, we get $(x_2^j-x_1^j)n_j^x+(y_2^j-y_1^j)n_j^y=0$. It stays:

$$\begin{aligned}
H_{ij} &= \int_0^1 -\frac{\sqrt{\gamma}}{2\pi r^2(s)}\Big((x_i-x_1^j)n_j^x+(y_i-y_1^j)n_j^y\Big)ds \\
&= -\frac{\sqrt{\gamma}}{2\pi}\Big((x_i-x_1^j)n_j^x+(y_i-y_1^j)n_j^y\Big)\int_0^1\frac{1}{r^2(s)}ds \\
&= -\frac{\sqrt{\gamma}}{2\pi}\Big((\vec{p}^{\,i}-\vec{p_1}^{\,j}).\vec{n}_j\Big)I_0
\end{aligned}$$

As written in section (2.2.4), D reachs zero if and only if $\vec{p_1}^{\,j}, \vec{p_2}^{\,j}$ and $\vec{p}^{\,i}$ are colinear, that is:

$$D=0 \qquad \Longleftrightarrow \qquad (\vec{p}^{\,i}-\vec{p_1}^{\,j}).\vec{n}_j=0$$

As I_0 is bounded (see section (C.1)), when $D = 0$, $H_{ij} = 0$.

To summarize, using the computation of I_0 detailled in section (C.1), we get:

$$\begin{array}{lll} \text{if } D < 0 & H_{ij} & = -\frac{\sqrt{\gamma}}{\pi\sqrt{-D}}\Big((\vec{p}^{\,i} - \vec{p_1}^{\,j}).\vec{n}_j\Big)\Big(arctan\Big(\frac{\beta+2\gamma}{\sqrt{-D}}\Big) - arctan\Big(\frac{\beta}{\sqrt{-D}}\Big)\Big) \\ \text{if } D = 0 & H_{ij} & = 0 \end{array}$$

Appendix B

Matrices computed for linear elements

The presented results are equivalent to those written in [10]. The notations used here are more adapted to an implementation with a loop on nodes instead of elements.

The integrated functions in G_{ij} and H_{ij} are always bounded, excepted when $\vec{p}_i$ is one of the ends of Γ_j. In the following, we will treat the general case first, then the specific terms.

B.1 Implementation to fill the matrices

We want to evaluate the values defined by eq.(2.28) and eq.(2.29):

$$G^1_{ij} = \int_{\Gamma_{e_1(j)}} u^*(\vec{x}_i, \vec{x})\phi_1(\vec{x})d\Gamma(\vec{x}) \qquad G^2_{ij} = \int_{\Gamma_{e_2(j)}} u^*(\vec{x}_i, \vec{x})\phi_2(\vec{x})d\Gamma(\vec{x})$$

$$H^1_{ij} = \int_{\Gamma_{e_1(j)}} v^*(\vec{x}_i, \vec{x})\phi_1(\vec{x})d\Gamma(\vec{x}) \qquad H^2_{ij} = \int_{\Gamma_{e_2(j)}} v^*(\vec{x}_i, \vec{x})\phi_2(\vec{x})d\Gamma(\vec{x})$$

Noting $\quad G^1_{ij} = G^1(P_i, \Gamma_{e_1(j)}) \quad$ and $\quad G^2_{ij} = G^2(P_i, \Gamma_{e_2(j)})$

we can write $\quad G^1_{in_1(j)} = G^1(P_i, \Gamma_j) \quad$ and $\quad G^2_{in_2(j)} = G^2(P_i, \Gamma_j) = G^1(P_i, -\Gamma_j).$

As a segment Γ_j is defined by his nodes $n_1(j)$ and $n_2(j)$, we can also note:

$$G^1_{in_1(j)} = G^1(P_i, n_1(j), n_2(j)) \qquad \text{and} \qquad G^2_{in_2(j)} = G^2(P_i, n_1(j), n_2(j)).$$

Then as illustrated in fig.(B.1), we get:

$$G^1_{in_1(j)} = G^1(P_i, n_1(j), n_2(j)) = G^2(P_i, n_2(j), n_1(j)).$$

So, by implementing carefully the filling of matrices G and H, we do not need to compute to explicit G^1 if we know G^2. Consequently, in the following of this appendix, we will only talk about G_{ij} which will stand for G^2_{ij}. Similarly for H.

Figure B.1: Two equivalent configurations with different shape functions.

B.2 Computation of G_{ij}

$$G_{ij} = \int_0^1 -\frac{ln(\alpha+\beta s+\gamma s^2)}{4\pi} s\sqrt{\gamma} ds$$

Integration by part:

$$\begin{array}{ll} f' = s & f = \frac{s^2}{2} \\ g = ln(\alpha+\beta s+\gamma s^2) & g' = \frac{\beta+2\gamma s}{\alpha+\beta s+\gamma s^2} \end{array}$$

$$\begin{aligned} G_{ij} &= -\frac{\sqrt{\gamma}}{4\pi}\Big(\Big[\frac{s^2}{2} ln(|\alpha+\beta s+\gamma s^2|)\Big]_0^1 - \int_0^1 \frac{s^2}{2}\frac{\beta+2\gamma s}{\alpha+\beta s+\gamma s^2} ds\Big) \\ &= -\frac{\sqrt{\gamma}}{8\pi}\Big(ln(|\alpha+\beta+\gamma|) - \int_0^1 \frac{\beta s^2+2\gamma s^3}{\alpha+\beta s+\gamma s^2} ds\Big) \end{aligned}$$

Let us define:

$$I_2 = \int_0^1 \frac{\beta s^2+2\gamma s^3}{\alpha+\beta s+\gamma s^2} ds$$

then we can write:

$$\begin{aligned} G_{ij} &= -\frac{\sqrt{\gamma}}{4\pi}\Big(\Big[\frac{s^2}{2} ln(|\alpha+\beta s+\gamma s^2|)\Big]_0^1 - \int_0^1 \frac{s^2}{2}\frac{\beta+2\gamma s}{\alpha+\beta s+\gamma s^2} ds\Big) \\ &= -\frac{\sqrt{\gamma}}{8\pi}\Big(ln(|\alpha+\beta+\gamma|) - I_2\Big) \end{aligned}$$

Using the computation of I_2 detailled in section (C.3), we have:

- If $D < 0$:

$$\begin{aligned} G_{ij} &= -\frac{\sqrt{\gamma}}{8\pi}\Bigg(ln(|\alpha+\beta+\gamma|) - 1 + \frac{\beta}{\gamma} - \frac{\beta^2 - 2\alpha\gamma}{2\gamma^2}\Big(ln(|\alpha+\beta+\gamma|) - ln(|\alpha|)\Big) \\ &\quad -\frac{\beta\sqrt{-D}}{\gamma^2}\Big(arctan\Big(\frac{\beta+2\gamma}{\sqrt{-D}}\Big) - arctan\Big(\frac{\beta}{\sqrt{-D}}\Big)\Big)\Bigg) \end{aligned}$$

- If $D = 0$:

$$G_{ij} = -\frac{\sqrt{\gamma}}{8\pi}\Bigg(ln(|\alpha+\beta+\gamma|) - 1 + \frac{\beta}{\gamma} - \frac{2\alpha}{\gamma} ln\Big(\Big|\frac{2\gamma}{\beta} + 1\Big|\Big)\Bigg)$$

- If $\vec{p_i} = \vec{p_1}$:

$$G_{ij} = -\frac{\sqrt{\gamma}}{8\pi}(ln(\gamma) - 1)$$

- If $\vec{p_i} = \vec{p_2}$:

$$G_{ij} = -\frac{\sqrt{\gamma}}{8\pi}(ln(\gamma) - 3)$$

B.3 Computation of H_{ij}

$$H_{ij} = \int_0^1 -\frac{\sqrt{\gamma}s}{2\pi r(s)} \vec{e_r}(s).\vec{n}_j^e ds$$

As computed in section (A.3), we have:

$$\vec{e_r}(s).\vec{n}_j^e = \frac{1}{r(s)}\Big((x_i - x_1^j)n_j^x + (y_i - y_1^j)n_j^y\Big)$$

So we can write:

$$\begin{aligned} H_{ij} &= \int_0^1 -\frac{\sqrt{\gamma}s}{2\pi r^2(s)}\Big((x_i - x_1^j)n_j^x + (y_i - y_1^j)n_j^y\Big) ds \\ &= -\frac{\sqrt{\gamma}}{2\pi}\Big((\vec{p}^{\,i} - \vec{p_1}^{\,j}).\vec{n}_j\Big) \int_0^1 \frac{s}{r^2(s)} ds \end{aligned}$$

$$\begin{aligned}\int_0^1 \frac{s}{r^2(s)}ds &= \int_0^1 \frac{1}{2\gamma}\frac{2\gamma s+\beta}{\alpha+\beta s+\gamma s^2}ds - \int_0^1 \frac{\beta}{2\gamma}\frac{1}{\alpha+\beta s+\gamma s^2}ds \\ &= \frac{1}{2\gamma}I_1 - \frac{\beta}{2\gamma}I_0\end{aligned}$$

- If $D<0$: I_0 and I_1 are well defined and we get:

$$\begin{aligned}H_{ij} &= -\frac{\sqrt{\gamma}}{2\pi}\Big((\vec{p}^{\,i}-\vec{p_1}^{\,j}).\vec{n}_j\Big)\Big(\frac{1}{2\gamma}I_1-\frac{\beta}{2\gamma}I_0\Big) \\ &= -\frac{\sqrt{\gamma}}{2\pi}\Big((\vec{p}^{\,i}-\vec{p_1}^{\,j}).\vec{n}_j\Big) \\ &\quad \Big(\frac{1}{2\gamma}\Big(ln(|\alpha+\beta+\gamma|)-ln(\alpha)\Big) \\ &\quad -\frac{\beta}{\gamma\sqrt{-D}}\Big(arctan\Big(\frac{\beta+2\gamma}{\sqrt{-D}}\Big)-arctan\Big(\frac{\beta}{\sqrt{-D}}\Big)\Big)\Big)\end{aligned}$$

- If $D=0$:

$$D=0 \qquad \Longleftrightarrow \qquad (\vec{p}^{\,i}-\vec{p_1}^{\,j}).\vec{n}_j=0$$

So for any $\vec{p_i}$ different from $\vec{p_1}$ and $\vec{p_2}$, we have:

$$H_{ij} = 0$$

When $\vec{p_i}$ is $\vec{p_1}$ or $\vec{p_2}$, I_1 is undetermined but we assume that $H_{ij}=0$.

Appendix C

Computation of integrals

$$I_0 = \int_0^1 \frac{1}{\alpha + \beta s + \gamma s^2} ds \qquad I_1 = \int_0^1 \frac{\beta + 2\gamma s}{\alpha + \beta s + \gamma s^2} ds \qquad I_2 = \int_0^1 \frac{\beta s^2 + 2\gamma s^3}{\alpha + \beta s + \gamma s^2} ds$$

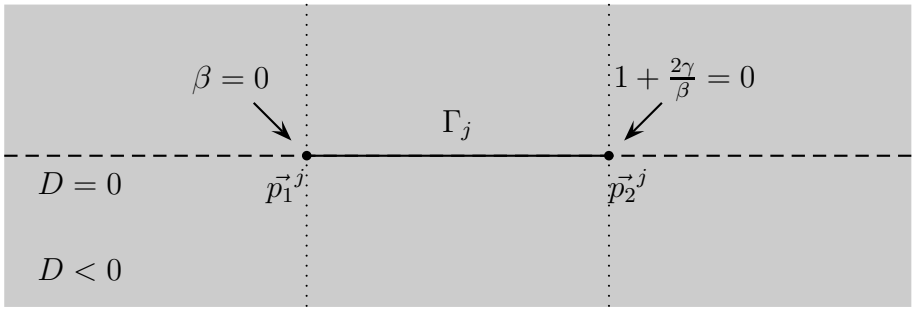

Figure C.1: Map of cases depending on the position of $\vec{p_i}$

C.1 Computation of I_0

As we have shown, $D \leq 0$ so we distinguish two cases.

When $D < 0$

$$I_0 = \frac{4\gamma}{-D} \int_0^1 \frac{1}{1 + \left(\frac{\beta + 2\gamma s}{\sqrt{-D}}\right)^2} ds$$

Change of variables:

$$t = \frac{\beta + 2\gamma s}{\sqrt{-D}} \qquad dt = \frac{2\gamma}{\sqrt{-D}} ds$$

$$\begin{aligned} I_0 &= \frac{4\gamma}{-D}\int_{\frac{\beta+2\gamma}{\sqrt{-D}}}^{\frac{\beta}{\sqrt{-D}}} \frac{\sqrt{-D}}{2\gamma}\frac{1}{1+t^2}dt \\ &= \frac{2}{\sqrt{-D}}\Big[arctan(t)\Big]_{\frac{\beta+2\gamma s}{\sqrt{-D}}}^{\frac{\beta}{\sqrt{-D}}} \\ &= \frac{2}{\sqrt{-D}}\Big[arctan\Big(\frac{\beta+2\gamma s}{\sqrt{-D}}\Big)\Big]_0^1 \\ &= \frac{2}{\sqrt{-D}}\Big(arctan\Big(\frac{\beta+2\gamma}{\sqrt{-D}}\Big) - arctan\Big(\frac{\beta}{\sqrt{-D}}\Big)\Big) \end{aligned}$$

This can be computed without any problem while $D \neq 0$. This case is treated in the next section.

When $D = 0$

Then we can write:

$$\alpha + \beta s + \gamma s^2 = \gamma(s + \frac{\beta}{2\gamma})^2$$

$$\begin{aligned} I_0 &= \int_0^1 \frac{1}{\gamma(s+\frac{\beta}{2\gamma})^2}ds \\ &= \frac{1}{\gamma}\Big[\frac{-1}{s+\frac{\beta}{2\gamma}}\Big]_0^1 \\ &= \frac{1}{\gamma}\Big(\frac{1}{\frac{\beta}{2\gamma}} - \frac{1}{1+\frac{\beta}{2\gamma}}\Big) \\ &= \frac{1}{\gamma\Big(1+\frac{\beta}{2\gamma}\Big)} \end{aligned}$$

I_0 is well defined only if $\beta \neq 0$ and $\frac{2\gamma}{\beta} + 1 \neq 0$. And assuming $D = 0$, we have:

$$\begin{cases} \beta = 0 \Leftrightarrow 4\alpha\gamma = 0 \Leftrightarrow \alpha = 0 \Leftrightarrow \|\vec{p_1} - \vec{p_i}\| = 0 \Leftrightarrow \vec{p_i} = \vec{p_1} \\ \frac{2\gamma}{\beta} + 1 = 0 \Leftrightarrow \beta = -2\gamma \Leftrightarrow \overrightarrow{p_1^j p_i} \cdot \overrightarrow{p_1^j p_2^j} = \|\overrightarrow{p_1^j p_2^j}\|^2 \Leftrightarrow \vec{p_i} = \vec{p_2} \end{cases} \tag{C.1}$$

We will take to treat those specific cases differently.

Limited development of I_0

Numerically, if D is very close to 0, then we handle huge quantities in I_0 due to the factor $\frac{1}{\sqrt{-D}}$. To avoid a deterioration of precision, we choose to write a limited development of the formula of I_0 for $D < 0$ which is used only for values of D close to 0.

Using the Taylor series expansion of arctan (valid for any real x such that $|x| < 1$):

$$arctan(x) = x - \frac{x^3}{3} + \frac{x^5}{5} + \cdots = \sum_{i=0}^{\infty} \frac{(-1)^i x^{2i+1}}{2i+1} \tag{C.2}$$

and the trigonometric law:

$$\forall x > 0, \qquad arctan(\frac{1}{x}) + arctan(x) = \frac{\pi}{2} \tag{C.3}$$

we get:

$$\forall x > 1, \qquad arctan(x) = \frac{\pi}{2} - \sum_{i=0}^{\infty} \frac{(-1)^i}{(2i+1)x^{2i+1}} \tag{C.4}$$

So for D close to 0 enough, we have $\frac{\beta+2\gamma}{\sqrt{-D}} > 1$ and $\frac{\beta}{\sqrt{-D}} > 1$ then we can write:

$$I_0 = \frac{2}{\sqrt{-D}}\Big(arctan\Big(\frac{\beta+2\gamma}{\sqrt{-D}}\Big) - arctan\Big(\frac{\beta}{\sqrt{-D}}\Big)\Big) \tag{C.5}$$

$$= \frac{2}{\sqrt{-D}}\Big(\frac{\pi}{2} - \sum_{i=0}^{\infty} \frac{(-1)^i(\sqrt{-D})^{2i+1}}{(2i+1)(\beta+2\gamma)^{2i+1}} - \frac{\pi}{2} + \sum_{i=0}^{\infty} \frac{(-1)^i(\sqrt{-D})^{2i+1}}{(2i+1)(\beta)^{2i+1}}\Big) \tag{C.6}$$

$$= 2\Big(-\sum_{i=0}^{\infty} \frac{(-1)^i(\sqrt{-D})^{2i}}{(2i+1)(\beta+2\gamma)^{2i+1}} + \sum_{i=0}^{\infty} \frac{(-1)^i(\sqrt{-D})^{2i}}{(2i+1)(\beta)^{2i+1}}\Big) \tag{C.7}$$

As $\sqrt{-D}$ is taken at the power $2i$ and $2i \geq 0$ for each $i \geq 0$, the computation is safe. In the implementation, the summation is done until the 20^{th} order.

C.2 Computation of I_1

Again, as $D \leq 0$ we distinguish two cases.

When $D < 0$

$$\begin{aligned} I_1 &= \int_0^1 \frac{\beta + 2\gamma s}{\alpha + \beta s + \gamma s^2} ds \\ &= \Big[ln(|\alpha + \beta s + \gamma s^2|)\Big]_0^1 \\ &= ln(|\alpha + \beta + \gamma|) - ln(\alpha) \end{aligned}$$

The computation is safe while $\alpha \neq 0$ and $|\alpha + \beta + \gamma| \neq 0$.

$$\begin{cases} |\alpha + \beta + \gamma| = r^2(1) = \|\vec{p_2} - \vec{p_i}\|^2 & \text{so } |\alpha + \beta + \gamma| = 0 \Leftrightarrow \vec{p_i} = \vec{p_2} \\ \alpha = r^2(0) = \|\vec{p_1} - \vec{p_i}\|^2 & \text{so } \alpha = 0 \Leftrightarrow \vec{p_i} = \vec{p_1} \end{cases} \tag{C.8}$$

In these two cases, the points $\vec{p_i}$,$\vec{p_1}$ and $\vec{p_2}$ are on line so $D = 0$. The case $D = 0$ is treated in the next section.

When $D = 0$

Then we can write:

$$\alpha + \beta s + \gamma s^2 = \gamma(s + \frac{\beta}{2\gamma})^2$$

$$\begin{aligned} I_1 &= \int_0^1 \frac{\beta + 2\gamma s}{\gamma(s + \frac{\beta}{2\gamma})^2} ds \\ &= \int_0^1 \frac{2}{\gamma(s + \frac{\beta}{2\gamma})} ds \\ &= \Big[2ln\Big(\Big|s + \frac{\beta}{2\gamma}\Big|\Big)\Big]_0^1 \\ &= \Big(ln\Big(\Big|1 + \frac{\beta}{2\gamma}\Big|\Big) - ln\Big(\Big|\frac{\beta}{2\gamma}\Big|\Big)\Big) \\ &= ln\Big(\Big|\frac{2\gamma}{\beta} + 1\Big|\Big) \end{aligned}$$

I_1 is well defined only if $\beta \neq 0$ and $\frac{2\gamma}{\beta} + 1 \neq 0$. And assuming $D = 0$, we have:

$$\begin{cases} \beta = 0 \Leftrightarrow 4\alpha\gamma = 0 \Leftrightarrow \alpha = 0 \Leftrightarrow \|\vec{p_1} - \vec{p_i}\| = 0 \Leftrightarrow \vec{p_i} = \vec{p_1} \\ \frac{2\gamma}{\beta} + 1 = 0 \Leftrightarrow \beta = -2\gamma \Leftrightarrow \overrightarrow{p_1^j p_i} \cdot \overrightarrow{p_1^j p_2^j} = \|\overrightarrow{p_1^j p_2^j}\|^2 \Leftrightarrow \vec{p_i} = \vec{p_2} \end{cases} \tag{C.9}$$

We will take to treat those specific cases differently.

C.3 Computation of I_2

$$I_2 = \int_0^1 \frac{\beta s^2 + 2\gamma s^3}{\alpha + \beta s + \gamma s^2} ds$$

Decomposition of the rationnal function:

$$\begin{aligned}
\frac{\beta s^2+2\gamma s^3}{\alpha+\beta s+\gamma s^2} &= 2s-\frac{2\beta s^2+2\alpha s}{\alpha+\beta s+\gamma s^2}+\frac{\beta s^2}{\alpha+\beta s+\gamma s^2}\\
&= 2s-\frac{\beta s^2}{\alpha+\beta s+\gamma s^2}-\frac{2\alpha s}{\alpha+\beta s+\gamma s^2}\\
&= 2s-\frac{\beta}{\gamma}+\frac{\beta}{\gamma}\frac{\beta s+\alpha}{\alpha+\beta s+\gamma s^2}-\frac{2\alpha s}{\alpha+\beta s+\gamma s^2}\\
&= 2s-\frac{\beta}{\gamma}+\Big(\frac{\beta^2}{\gamma}-2\alpha\Big)\frac{1}{2\gamma}\frac{2\gamma s+\beta}{\alpha+\beta s+\gamma s^2}\\
&\quad -\frac{\beta}{2\gamma}\Big(\frac{\beta^2}{\gamma}-2\alpha\Big)\frac{1}{\alpha+\beta s+\gamma s^2}+\frac{\alpha\beta}{\gamma}\frac{1}{\alpha+\beta s+\gamma s^2}\\
&= 2s-\frac{\beta}{\gamma}+\frac{\beta^2-2\alpha\gamma}{2\gamma^2}\frac{2\gamma s+\beta}{\alpha+\beta s+\gamma s^2}+\frac{\beta}{\gamma}\Big(2\alpha-\frac{\beta^2}{\gamma}\Big)\frac{1}{\alpha+\beta s+\gamma s^2}\\
&= 2s-\frac{\beta}{\gamma}+\frac{\beta^2-2\alpha\gamma}{2\gamma^2}\frac{\beta+2\gamma s}{\alpha+\beta s+\gamma s^2}-\frac{\beta D}{2\gamma^2}\frac{1}{\alpha+\beta s+\gamma s^2} \qquad \text{(C.10)}
\end{aligned}$$

So we have:

$$\begin{aligned}
I_2 &= \Big[s^2-\frac{\beta}{\gamma}s\Big]_0^1+\frac{\beta^2-2\alpha\gamma}{2\gamma^2}I_1-\frac{\beta D}{2\gamma^2}I_0\\
&= 1-\frac{\beta}{\gamma}+\frac{\beta^2-2\alpha\gamma}{2\gamma^2}I_1-\frac{\beta D}{2\gamma^2}I_0
\end{aligned}$$

I_1 and I_0 are well defined when $D<0$. When $D=0$, they are well defined only if $\beta\neq 0$ and $\frac{2\gamma}{\beta}+1\neq 0$. Those cases are treated in the next two sections.

When $\vec{p_i}=\vec{p_1}$ (special case of $D=0$)

In this case, $\alpha=0$ and $\beta=0$ so we have:

$$I_2=\int_0^1\frac{2\gamma s^3}{\gamma s^2}ds=\int_0^1 2sds=\Big[s^2\Big]_0^1=1$$

When $\vec{p_i}=\vec{p_2}$ (special case of $D=0$)

In this case, $\beta=-2\gamma$ so we have:

$$\begin{aligned}
I_2 &= \int_0^1\frac{-2\gamma s^2+2\gamma s^3}{\alpha+\beta s+\gamma s^2}ds\\
&= 2\gamma\int_0^1 s^2\frac{s-1}{\alpha+\beta s+\gamma s^2}ds
\end{aligned}$$

Since $D = 0$ we can write :

$$\alpha + \beta s + \gamma s^2 = \gamma(s + \frac{\beta}{2\gamma})^2 = \gamma(s-1)^2$$

so we get:

$$\begin{aligned} I_2 &= 2\gamma \int_0^1 s^2 \frac{s-1}{\gamma(s-1)^2} ds \\ &= 2\int_0^1 \frac{s^2}{s-1} ds \end{aligned}$$

Decomposition of the rationnal function:

$$\begin{aligned} \frac{s^2}{s-1} &= s\Big(\frac{s-1}{s-1} + \frac{1}{s-1}\Big) \\ &= s + \frac{s}{s-1} \\ &= s + 1 + \frac{1}{s-1} \end{aligned}$$

Then we have:

$$\begin{aligned} I_2 &= 2\int_0^1 s + 1 + \frac{1}{s-1} ds \\ &= 2\Big[\frac{s^2}{2} + s + ln(s-1)\Big]_0^1 \\ &= 2\Big(\frac{1}{2} + 1\Big) \\ &= 3 \end{aligned}$$

Appendix D

Analytical solutions

D.1 Cases with rotational symmetry

Working with cylindrical coordinates of center $\vec{O}$ (the center of the disc), the initial equation $\Delta u = 0$ applied to a disc of radius R becomes:

$$\forall r \in]0, R], \forall \theta \in [0, 2\pi], \qquad \frac{\partial^2 u(r,\theta)}{\partial r^2} + \frac{1}{r}\frac{\partial u(r,\theta)}{\partial r} + \frac{1}{r^2}\frac{\partial^2 u(r,\theta)}{\partial \theta^2} = 0$$

Here, the symmetry of the problem brings $u(r, \theta) = u(r)$. So we get:

$$\forall r \in]0, R], \qquad \frac{\partial^2 u(r)}{\partial r^2} + \frac{1}{r}\frac{\partial u(r)}{\partial r} = 0$$

Writing $v(r) = \frac{\partial u(r)}{\partial r}$ and $v'(r) = \frac{\partial^2 u(r)}{\partial r^2}$, we have to solve:

$$\forall r \in]0, R], \qquad v'(r) + \frac{1}{r}v(r) = 0 \tag{D.1}$$

Let us remark that $v_1(r) = \frac{\alpha}{r}$ with α constant, is a particular solution of eq.(D.1). Now, let suppose that there exists another solution v_2. We introduce f such that $v_2(r) = f(r)\frac{\alpha}{r}$. We compute its derivative:

$$\forall r \in]0, R], \qquad v_2'(r) = -\frac{\alpha}{r^2}f(r) + \frac{\alpha}{r}f'(r) \tag{D.2}$$

and then we get:

$$\begin{aligned}
\forall r \in]0, R], \qquad v_2'(r) + \frac{1}{r}v_2(r) &= 0 && \text{(D.3)}\\
-\frac{\alpha}{r^2}f(r) + \frac{\alpha}{r}f'(r) + \frac{\alpha}{r^2}f(r) &= 0 && \text{(D.4)}\\
\frac{\alpha}{r}f'(r) &= 0 && \text{(D.5)}\\
f'(r) &= 0 && \text{(D.6)}\\
& && \text{(D.7)}
\end{aligned}$$

So f needs to be constant. So when α describes $\mathbb{R}$, $v(r) = \frac{\alpha}{r}$ describes all the solutions of eq.(D.1). By integrating, we obtain all the solutions u:

$$\forall r \in]0, R], \qquad u(r) = \alpha ln(r) + \beta \tag{D.8}$$

D.1.1 Analytical solution for a disc

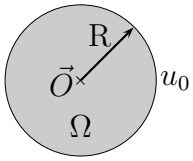

Figure D.1: Boundary conditions on a disc

As u is continuous on the domain Ω and $r \mapsto ln(r)$ is not bounded in the neighboorhood of $r = 0$, we necessarily get $\alpha = 0$. So u has to be constant on the whole domain. Then, given the boundary condition $u(R) = u_0$, we deduce:

$$\forall \mathbf{x} \in \Omega, \qquad u(\mathbf{x}) = u_0 \tag{D.9}$$

D.1.2 Analytical solution for a crown

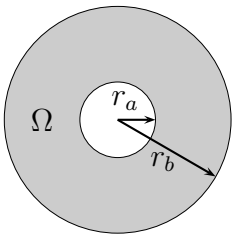

Figure D.2: Boundary conditions on a crown

As there is the same symmetry, we get eq.(D.8) again. This time, the center point does not belong to the domain so α is not necessarily zero. The two constants α and β are fixed by the boundary conditions.

Dirichlet boundary conditions only

Considering that we have to satisfy:

$$u(r_a) = a \qquad and \qquad u(r_b) = b \tag{D.10}$$

we can compute α and β:

$$\alpha = \frac{b-a}{ln(r_b) - ln(r_a)} \qquad and \qquad \beta = \frac{aln(r_b) - bln(r_a)}{ln(r_b) - ln(r_a)} \tag{D.11}$$

Mixed boundary conditions

Considering that we have to satisfy:

$$u(r_a) = a \qquad and \qquad v(r_b) = b \tag{D.12}$$

we can compute α and β:

$$\alpha = br_b \qquad and \qquad \beta = a - \alpha ln(r_a) = a - br_b ln(r_a) \tag{D.13}$$

So we get:

$$u(r) = br_b ln\Big(\frac{a}{r_a}\Big) + a \tag{D.14}$$

D.2 Cases equivalent to a 1D problem

In this section, we study the case of a rectangle to which we impose boundary conditions such that on two opposite sides, the normal flux is zero and on the two other sides, the field is given. This way, the field is invariant in one direction (let say $\vec{e}_y$ like in fig.(D.3)) and the problem is equivalent to a 1D case meaning $u = u(x)$. This yields:

$$\Delta u = \frac{\partial^2 u}{\partial x^2} + \frac{\partial^2 u}{\partial y^2} + \frac{\partial^2 u}{\partial z^2} = \frac{\partial^2 u}{\partial x^2}$$

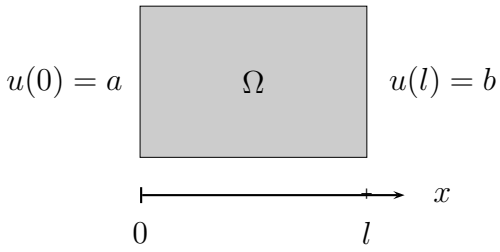

Figure D.3: Boundary conditions on a rectangle

Then the initial equation $\Delta u = 0$ applied to this rectangle becomes:

$$\forall x \in [0, l], \qquad \frac{\partial^2 u}{\partial x^2} = 0$$

So the solution field is written:

$$u(x) = \alpha x + \beta \qquad \text{and} \qquad v(x) = \alpha \qquad \text{where} \qquad \begin{cases} \beta = a \\ \alpha = \frac{1}{l}(b-a) \end{cases} \tag{D.15}$$

Bibliography

[1] W.-T. Ang. *A beginner's course in boundary element methods*. Boca Raton, FL : Universal Publishers, 2007.

[2] K. Bertram Broberg. *Crack and fractures*. Academic Press, 1999.

[3] C.A. Brebbia and J. Dominguez. *Boundary Elements An Introductory Course*. Computational Mechanics Publications McGraw-Hill Book Company, 1992.

[4] H.D. Bui and A. Ehrlacher. Mécanique des solides anélastiques. *C. R. Acad. Sc. Paris*, 290(B):273–276, 1980.

[5] S. Chaillat. *Fast Multipole Method for 3-D elastodynamic boundary integral equations. Application to seismic wave propagation.* Phd. thesis, École Nationale des Ponts et Chaussées, 2009.

[6] S. De Leon. *The Boundary Element Method for Linear Acoustic Systems*. Phd. thesis, Schulich School of Music McGill University, 2008.

[7] R.A. Eubanks and E. Sternberg. On the completeness of the boussinesq-papkovich stress functions. *J. Rat. Mech. Anal.*, 5(5):735–746, 1956.

[8] B. Fedelich and A. Ehrlacher. Sur un principe de minimum concernant des matériaux à comportement indépendant du temps physique. *C. R. Acad. Sc. Paris*, 308(II):1391–1394, 1989.

[9] B. Fedelich and A. Ehrlacher. An analysis of stability of equilibrium and of quasi-statis transformations on the basis of the dissipation fucntion. *European journal of mechanics, A/Solids*, 16(5):833–855, 1997.

[10] J. Friedrich. A linear analytical boundary element method for 2d homogeneous potential problems. *Computers and Geosciences*, 28(5):679–692, 2002.

[11] J.L. Hess and A.M.O. Smith. *Calculation of Potential Flow about Arbitrary Bodies*, volume 8. Ed.D.Kuchemann, Pergamon Press, London, 1967.

[12] M. Jaswon. Integral equation methos in potential theory. *Proc. Roy. Soc. Ser. A.*, 275:23–32, 1963.

[13] N. Moës. *Application de la méthode des éléments de frontière au calcul des pièces fissurées*. Travail de fin d'études, Université de Liège, 1992.

[14] N. Moës, N. Chevaugeon, and F. Dufour. A regularized brittle damage model solved by a level set technique.

[15] K.V. Nguyen. *Etude des effets de site dus aux conditions topographiques et géotechniques par une méthode hybride éléments finis/éléments frontières*. Phd. thesis, École Nationale des Ponts et Chaussées, 2005.

[16] Q.S. Nguyen, R.M. Pradeilles, and C. Stolz. Sur une loi de propagation régularisante en rupture et endommagement fragile. *C. R. Acad. Sc. Paris*, 309(II):1515–1520, 1989.

[17] E. Premat. *Prise en compte d'effets météorologiques dans un méthode d'éléments finis de frontière*. Phd. thesis, Ecole Nationale des Travaux Publics de l'Etat, 2000.

[18] F.J. Rizzo. An integral equation approach to boundary value problems of classical elastostatics. *Quaterly of Applied Mathematics*, 25:83, 1967.

[19] D. Salac and W. Lu. A level set approach to model directed nanocrack patterns. *Computational Materials Science*, 39:849–856, 2007.

[20] E. Taroco. Shape sensitivity analysisi in linear elastic fracture mechanics. *Comput. Methods Appl. Mech. Engrg.*, 188:697–712, 2000.

[21] L.A. Vese and T.F. Chan. A multiphase level set framework for image segmentation using the mumford and shah model. *International Journal of Computer Vision*, 50(3):271–293, 2002.